AD-A137 827 LASER CHEMICAL VAPOR DEPOSITION(U) UNIVERSITY OF SOUTHERN CALIFORNIA LOS ANGELES CENTER FOR LASER STUDIES S D ALLEN ETAAL. 20 DEC 83 AFOSR-TR-84-0052 1/1

UNCLASSIFIED AFOSR-79-0135 F/G 20/5 NL

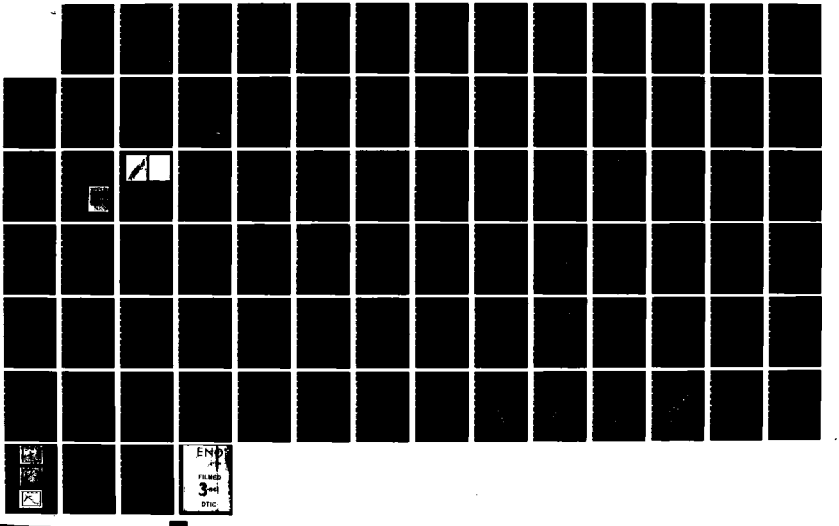

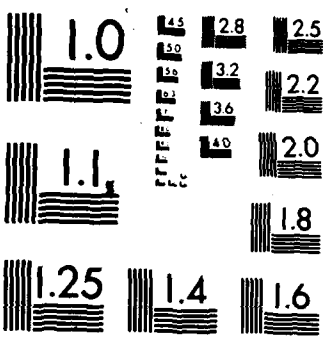

MICROCOPY RESOLUTION TEST CHART
NATIONAL BUREAU OF STANDARDS-1963-A

Scientific Report

AFOSR-79-0135

LASER CHEMICAL VAPOR DEPOSITION

By

Susan D. Allen and Michael Bass

December 20, 1983

Center for Laser Studies
University of Southern California
Los Angeles, California 90089-1112

TABLE OF CONTENTS

SECURITY CLASSIFICATION OF THIS PAGE (When Data Entered)

REPORT DOCUMENTATION PAGE	READ INSTRUCTIONS BEFORE COMPLETING FORM
1. REPORT NUMBER: AFOSR-TR- 84-0052	2. GOVT ACCESSION NO.
3. RECIPIENT'S CATALOG NUMBER	
4. TITLE (and Subtitle): Laser Chemical Vapor Deposition	5. TYPE OF REPORT & PERIOD COVERED: Final Scientific Report
6. PERFORMING ORG. REPORT NUMBER	
7. AUTHOR(s): Susan D. Allen and Michael Bass	8. CONTRACT OR GRANT NUMBER(s): AFOSR-79-0135
9. PERFORMING ORGANIZATION NAME AND ADDRESS: Center for Laser Studies, University of Southern California, Los Angeles, CA 90089-1112	10. PROGRAM ELEMENT, PROJECT, TASK AREA & WORK UNIT NUMBERS: 61102F, 2301/A1
11. CONTROLLING OFFICE NAME AND ADDRESS: AFOSR, Bolling AFB, D. C. 20332 - NP	12. REPORT DATE: Dec. 20, 1983
	13. NUMBER OF PAGES: 83
14. MONITORING AGENCY NAME & ADDRESS (if different from Controlling Office)	15. SECURITY CLASS. (of this report): Unclassified
	15a. DECLASSIFICATION/DOWNGRADING SCHEDULE

16. DISTRIBUTION STATEMENT (of this Report)

Approved for public release; Distribution unlimited

17. DISTRIBUTION STATEMENT (of the abstract entered in Block 20, if different from Report)

18. SUPPLEMENTARY NOTES

19. KEY WORDS (Continue on reverse side if necessary and identify by block number)

20. ABSTRACT (Continue on reverse side if necessary and identify by block number)

Metal, dielectric and semiconductor films have been deposited by laser chemical vapor deposition (LCVD) using both pulsed and cw laser sources on a variety of substrates. For LCVD on substrates such as quartz, the deposition was monitored optically in both transmission and reflection using a collinear visible laser and the depositing CO_2 laser. Deposition initiation and rate were correlated with irradiation conditions, the laser

DD FORM 1 JAN 73 1473 EDITION OF 1 NOV 65 IS OBSOLETE

UNCLASSIFIED

SECURITY CLASSIFICATION OF THIS PAGE (When Data Entered)

AFOSR-TR- 84-0052

generated surface temperature, and the changing optical properties of the film/substrate during deposition. Single crystallites of W greater than 100 μm tall were deposited using a Kr laser on Si substrates.

INTRODUCTION

Under this program we have investigated a wide range of laser chemical vapor deposition (LCVD) reactions (Table 1) on metallic, semiconductor and insulator substrates using pulsed and cw infrared and visible lasers. Not all of the reactions given in Table 1 yielded good results under the conditions used in the preliminary survey. For example, the LCVD films from the metal alkyls were heavily oxidized due to the poor vacuum conditions employed in the early work. In order to concentrate on the characteristics unique to LCVD, only those systems which yielded films of good quality under a wide range of conditions such as the metal carbonyls and the H_2 reduction of WF_6 were emphasized.

TABLE 1

$Ni(CO)_4$ ---------- Ni + CO

$WF_6 + H_2$ ---------- W + HF

$W(CO)_6$ ---------- W + CO

$Fe(CO)_5$ ---------- Fe + CO

$Al(CH_3)_3$ $\xrightarrow{(H_2)}$ Al + CH_4

$Sn(CH_3)_4$ ---------- Sn + CH_4

$TiCl_4 + H_2 + CO_2$ ---------- TiO_2 + HCl + CO

$TiCl_4 + CH_4$ $\xrightarrow{(H_2)}$ TiC + HCl

$TiCl_4 + C_2H_2 + H_2$ ---------- TiC + HCl

$Ga(CH_3)_3 + As(CH_3)_3$ ---------- GaAs + CH_4

EXPERIMENTAL APPARATUS

The cw CO_2 LCVD apparatus is shown in Fig. 1. Similar optical arrangements are used for LCVD with the pulsed CO_2 and cw Kr lasers. The laser is an electrically pulsed, line tunable cw CO_2 with maximum output power of 40 W. Attenuation of the beam is provided by current control and a wire grid polarizer. A removable power meter and/or fluorescent viewing plates are used to check power stability and beam quality. A He-Ne beam is folded into the optical path with a ZnSe Brewster angle beam splitter to allow optical monitoring of the thickness of the LCVD film. Both beams are focused through a NaCl widnow onto the substrate with a 10 in. focal length 10.6 μm Ar-coated ZnSe lens. The CO_2 beam profile at the substrate was measured by pinhole scans and is approximately gaussian with a D_{1/e^2} = 600 μm. The beam diameter of the He-Ne laser at the focus is much smaller. The temporal intensity profile of the CO_2 pulses of several ms or longer was essentially a step function with some initial overshoot as measured using a HgCdTe detector. Because the amount of reactant used during LCVD is a small fraction of the total concentration, the depositions were carried out with closed reaction cells. Fused quartz is an excellent substrate material for LCVD using a CO_2 laser as it has a high absorption coefficient at 10.6 μm and is transparent in the visible for ease of optical monitoring, both visually and with the He-Ne laser. In addition, quartz has a low thermal conductivity which tends to further localize the deposition and a high resistance to thermal stress.

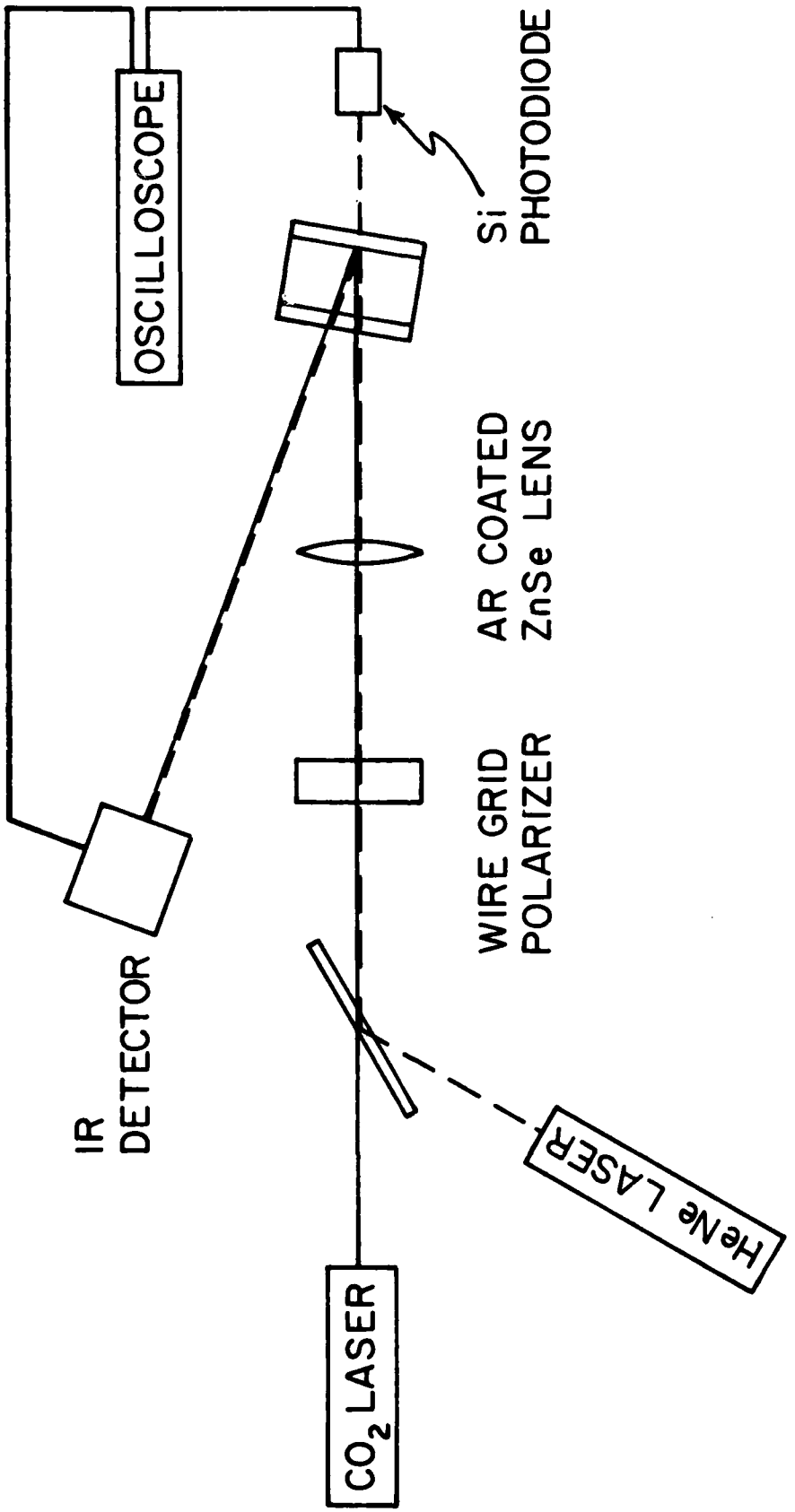
OSCILLOSCOPE
Si
PHOTODIODE
AR COATED
ZnSe LENS
WIRE GRID
POLARIZER
IR
DETECTOR
HeNe LASER
CO_2 LASER

FIGURE 1

RESOLUTION ENHANCEMENT

For most of the films deposited using the above apparatus, the deposition profile thickness for "short" irradiation times is a truncated gaussian shape and reflects the temperature profile generated by the gaussian laser beam on the substrate. The diameter of the deposit can be much less than the corresponding beam diameter, however, because the deposition rate is a highly nonlinear, usually exponential, function of the substrate temperature. The result is a deposit thickness profile which has the shape of the central portion of a gaussian curve. This "resolution enhancement" effect is also observed in other laser deposition methods to some degree. LCVD spot diameters as small as 1/10 of the laser beam diameter have been observed. The thickness profile for these "long" irradiation times changes smoothly from the truncated gaussian to a double humped "volcano" shape. As the laser intensities used are not sufficient to melt either quartz or Ni and no evidence of melting is observed, the cange in profile is ascribed to a depletion of reactants and build up of products at the center for the irradiated area and entrainment of reactants from the edges.

OPTICAL SELF-LIMITING

For most metal films deposited by LCVD on highly absorbing substrates such as SiO_2 at 10.6 μm, the deposition rate decreases as the film is deposited if a constant intensity irradiation is used. This "optical self-limiting" occurs because as the reflective metal film is deposited on an absorbing substrate, the amount of laser energy and therefore the substrate temperature decreases and the deposition rate also decreases. In extreme cases, depending on the thermodynamics and kinetics of the deposition reaction, the deposition rate can approach zero after the deposition of some critical thickness. A plot, therefore, of the "average deposition rate", defined as the LCVD film thickness divided by the irradiation time, usually yields a decreasing function with increasing irradiation time.

In order to understand and quantify this behavior, the apparatus in Fig. 1 was used to measure the LCVD film thickness optically by monitoring the He-Ne intensity during deposition. The initial results established the qualitative behavior of such LCVD reactions. During the first part of the irradiation, the transmitted He-Ne intensity does not change (cf. Fig. 2), i.e., no deposition takes place. This corresponds to the time necessary to heat the substrate to the deposition temperature. At some point, the He-Ne transmission decreases rapidly and essentially bottoms out. Depending on the irradiation time, the final transmission may or may not be effectively zero. In order to obtain more quantitative information on the deposition

rate as a function of time, it has been necessary to digitize the oscilloscope photos and iteratively calculate the deposition rate using the slopes and absolute values of the transmission curves and the Fresnel equations. This data analysis has been accomplished after the completion of the AFOSR program. Figure 2 is an example of the digitized He-Ne transmission curve and Fig. 3 is the corresponding deposition rate as a function of irradiation time.

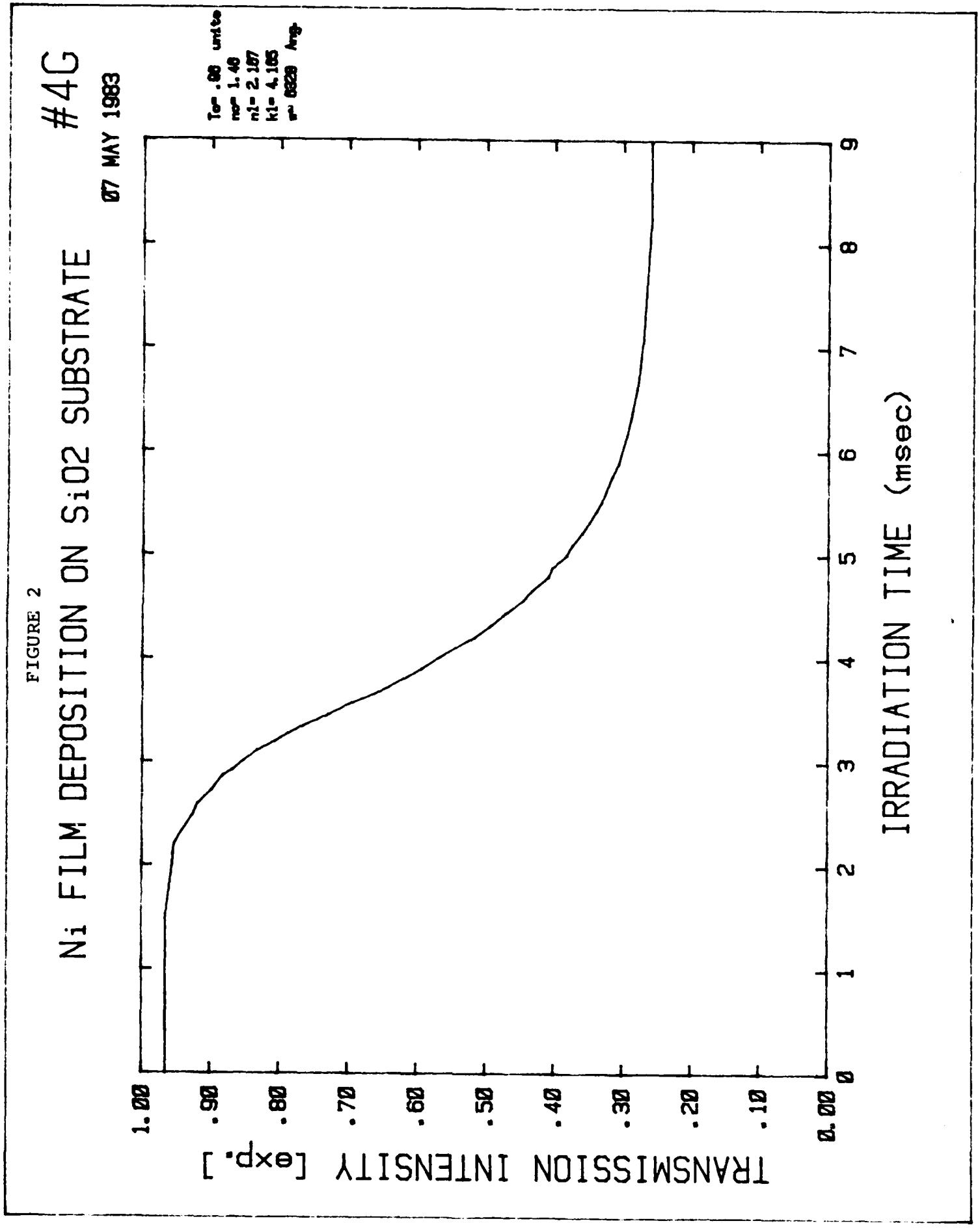
Ni FILM DEPOSITION ON SiO2 SUBSTRATE
#4C
07 MAY 1983
TRANSMISSION INTENSITY [exp.]
IRRADIATION TIME (msec)
1.00
.90
.80
.70
.60
.50
.40
.30
.20
.10
0.00
0
1
2
3
4
5
6
7
8
9

FIGURE 2

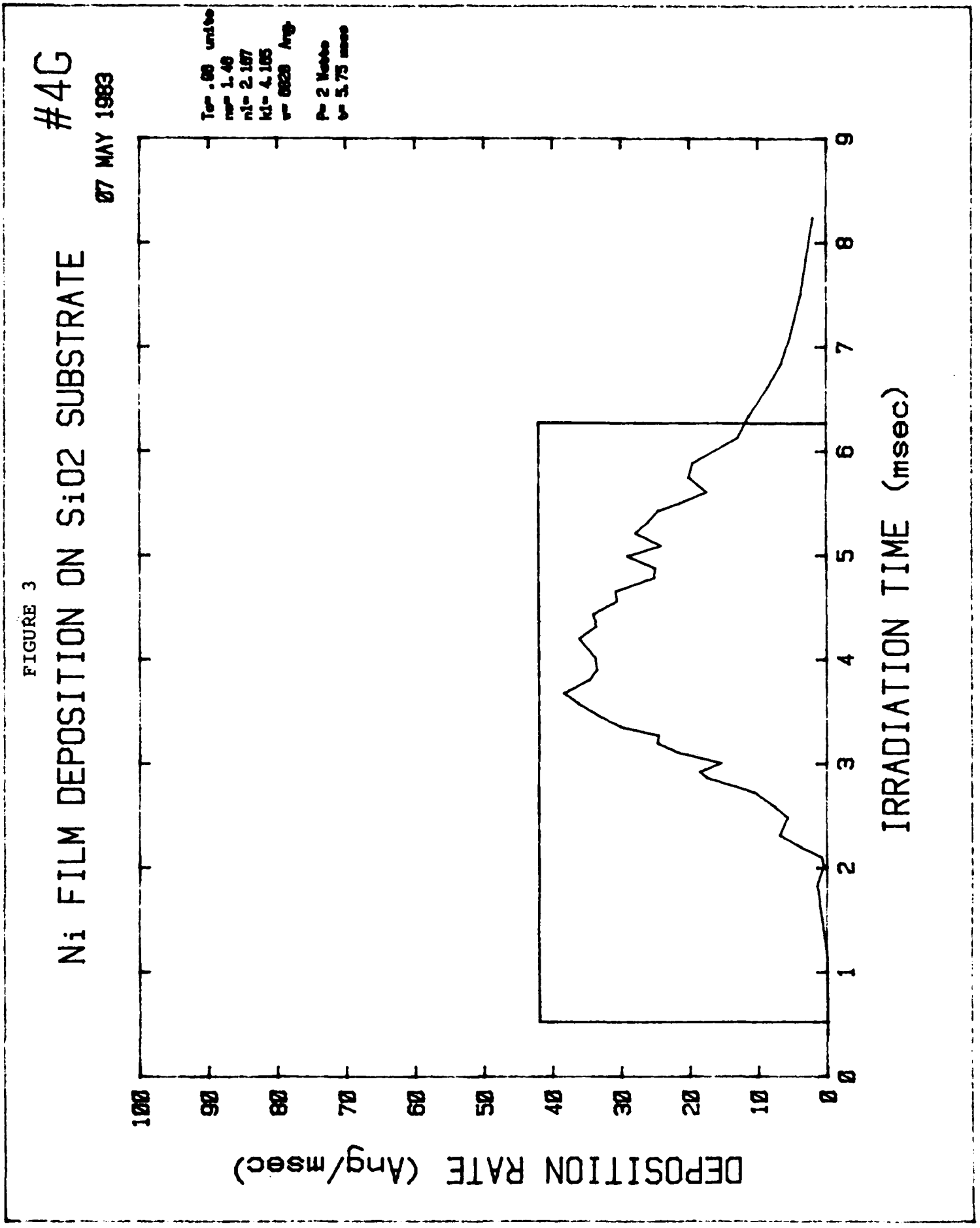
#4G
07 MAY 1983
Ni FILM DEPOSITION ON SiO2 SUBSTRATE
DEPOSITION RATE (Ang/msec)
IRRADIATION TIME (msec)
0
10
20
30
40
50
60
70
80
90
100
1
2
3
4
5
6
7
8
9

FIGURE 3

PULSED LCVD

Another approach to simplifying the complex deposition rate behavior exhibited by LCVD of reflective films on absorbing substrates is to use a laser pulse shorter than the time it takes for significant deposition to take place. Using a CO_2 TEA laser with a 1 μsec pulse alength, a large increase in surface temperature can be generated which then decays with a time constant on the order of milliseconds. The deposition of, for example, Ni from $Ni(CO)_4$ is again monitored optically using a colinear He-Ne beam. Instead of the expected single intensity decay curve, two separate decay curves are observed for the higher energy laser pulses and neither is simple. For low energies, there is an induction period before deposition begins. At higher energies, an initial deposition takes place, but deposition stops and then continues after a delay time. The total LCVD film thickness scales with the incident energy with maximum thickness achieved before damage to the substrate of several hundred Å. Preliminary pulsed LCVD results using the system Fe from $Fe(CO)_5$ yielded transmission vs. time curves with only one decay region.

Although there is some contribution to the initial decay region observed for pulsed LCVD $Ni(CO)_4$ from defocusing of the He-Ne beam due to the creation of a thermal lens in the laser heated substrate, this effect alone does not explain the deposition behavior. Similar induction times have been observed using cw laser irradiaiton at relatively high powers on a msec time scale.

LASER HEATED TEMPERATURE CALCULATIONS

In irder to understand the LCVD rate as a function of irradiation time, in particular, the time and the resolution enhancement effects discussed earlier at which reaction initiation takes place, the laser generated surface temperature profile must be known. Methods of measuring surface temperature on a submillisecond time scale and micron spatial scale do not currently exist and we are therefore forced to rely on theoretical calculations calibrated with experimental data such as the time needed to melt a substrate at a specific intensity and intensity profile. Such calculations are not simple because the thermal and presumably also the optical properties of the substrate vary with temperature even in the absence of the complications introduced by the LCVD film.

Iterative calculations of the surface temperature as a function of irradiation time were performed and the results are sown in Fig. 4. These curves are qualitativly reasonable and correlate well with the experimental data, but make several assumptions which are not valid. In particular, it is assumed that the thermal properties change uniformly throughout the substrate although the temperature does not. Numerical integration calculations are under way to remove most of these restrictions.

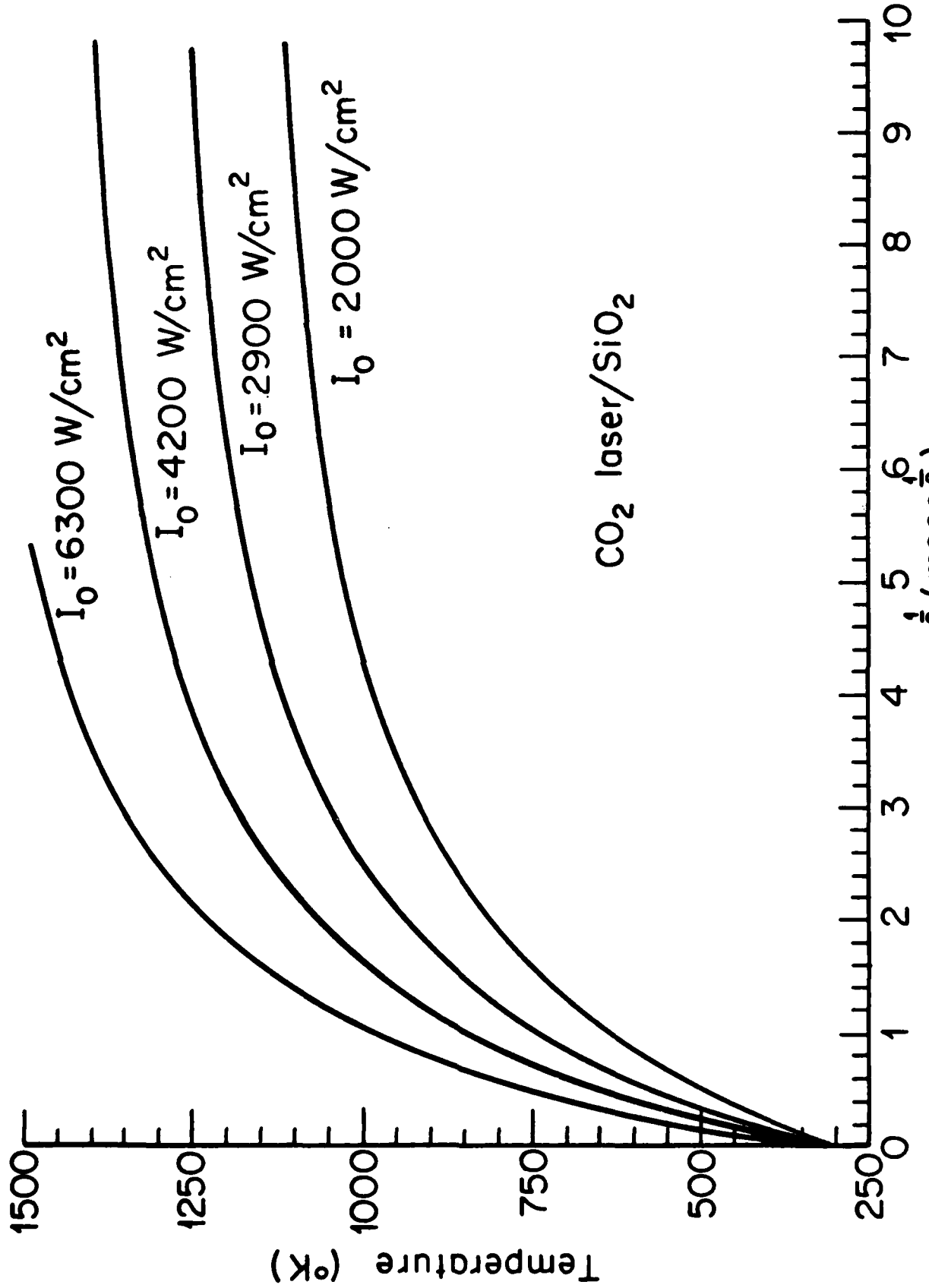
Temperature (°K)
1500
1250
1000
750
500
250
0
1
2
3
4
5
6
7
8
9
10
$\tau^{\frac{1}{2}}$ (msec$^{\frac{1}{2}}$)
I_o=6300 W/cm^2
I_o=4200 W/cm^2
I_o=2900 W/cm^2
I_o = 2000 W/cm^2
CO_2 laser/SiO_2

FIGURE 4

LCVD W/Si

W films were deposited on Si substrates using a Kr laser source and $WF_6 + H_2$ reactants. A curious growth pattern was observed for some spot depositions. Single crystal W spikes could be deposited with dimensions on the order of 40 - 50 μm wide and 50 - 120 μm tall. These are similar in geometry to the polycrystalline C and Si rods deposited by LCVD by Bauerle* et.al., but the appearance of one or at most a few large crystals has not previously been observed. The growth rates measured for these crystallites approach a mm/sec. Such structures have not been observed for LCVD W on SiO_2 using the CO_2 laser for similar reactant concentrations. It appears that the difference in growth habit is related to the large difference in the laser heated areas in the two cases. Examination of a LCVD W spot on Si where single crystal growth did not take place reveals the familiar "volcano" shape observed in LCVD with the CO_2/SiO_2 system. In the center of the volcano are small crystallites which are miniature versions of the large single crystal. Because the Kr laser irradiates an area on the order to 10 μm as opposed to the hundreds of microns irradiated by the CO_2 laser, it is possible for one or several of these crystallites to dominate the growth. (LCVD W spikes have been deposited with 1 - 4 crystallites apparent in the SEM photographs.)

* (Appl. Phys. Lett. 40, 819 (1982)).

STUDENT SUPPORT

M.S. degrees in Materials Science were awarded to two students supported by this program: A. B. Trigubo and Y.-C. Liu. Their names appear on several of the publications listed herein. In addition, an undergraduate work-study student, S. Mazuk, was also supported. He will graduate with a B.S. degree in Physics in June 1984 and plans to pursue graduate study in a field related to the work he has done under AFOSR sponsorship.

CONTINUED RESEARCH

Work in LCVD will continue under the sponsorship of several agencies. DOE is funding a program which has as its goal the increased understanding of the limiting processes in LCVD such as the optical effects discussed previously, diffusion and convection. Semiconductor Research Corporation is funding further work on small spot size deposition of metallic or semiconducting films with the technological goal of repair of transparent microfaults in VLSIC masks.

Publications

1. Laser Chemical Vapor Deposition - Applications in Materials Processing, S. D. Allen, Proceedings of the SPIE 198, (1980).

2. Laser Chemical Vapor Deposition of Titanium Carbide, J. Mazumder and S. D. Allen, Proceedings of the SPIE 198, (1980).

3. Laser Chemical Vapor Deposition, S. D. Allen, in "Physical Processes in Laser-Materials Interactions," ed. M. Bertolotti, Plenum Press, NY (1982).

* 4. Laser Chemical Vapor Deposition - A Technique for Selective Area Deposition, S. D. Allen, J. Appl. Phys. 52, 6501 (1981).

5. Laser Chemical Vapor Deposition, S. D. Allen, A. B. Trigubo, and Y.-C. Liu, Proceedings of the Eighth International Conference on Chemical Vapor Deposition, Electrochemical Society 81-7, 267 (1981).

6. Laser CVD of Metal Films Using Both Pulsed and CW Lasers, S. D. Allen, Y.-C. Liu, and A. B. Trigubo, J. Opt. Soc. Am. 71, 1575 (1981).

* 7. Properties of Several Types of Films Deposited by Laser CVD, S. D. Allen and A. B. Trigubo, J. Vac. Sci. Tech. 20, 469 (1982).

8. Laser Deposition, Susan D. Allen, Photonics Spectra 1982 (1) 54.

* 9. Laser CVD of Selected Area Fe and W Films, S. D. Allen and A. B. Trigubo, J. Appl. Phys. 54, 1641 (1983).

*10. Direct Writing Using Laser Chemical Vapor Deposition, S. D. Allen, A. B. Trigubo, and R. Y. Jan, Proceedings of the Materials Research Society Symposia, Volume 17.

*11. Laser Chemical Vapor Deposition, S. D. Allen, Proceedings of the 19th University Conference on Ceramic Science.

*12. Laser Chemical Vapor Deposition Using Pulsed and CW Lasers, S. D. Allen, A. B. Trigubo, and Y.-C. Liu, to be published in Optical Engineering.

13. "Laser Deposition and Etching", S. D. Allen, chapter in Physics of Thin Films series, in preparation (Academic Press).

* Reprints included.

Oral Papers (1980-1983)

1. Selected Area Deposition Using Laser CVD
   S. D. Allen and A. B. Trigubo
   American Vacuum Society
   Detroit, Michigan (10/80)

* 2. Laser Chemical Vapor Deposition
   S. D. Allen
   Western Metal and Tool Conference
   Los Angeles, CA (3/81)

3. Characteristics of Laser CVD Films
   S. D. Allen and A. B. Trigubo
   International Conference on Metallurgical Coatings
   San Francisco, CA (4/81)

* 4. Laser CVD - A Technique for Selective Area Deposition
   A. B. Trigubo and S. D. Allen
   Southern California American Vacuum Society
   Anaheim, CA (4/81)

5. Laser CVD - Applications to Selected Area Deposition
   Susan D. Allen
   Workshop on the Intera-tion of Laser Radiation with Surfaces
   for Applications to Microelectronics
   Massachusetss Institute of Technology
   Boston, MA (5/81)

6. Laser CVD of Metal Films Using Both Pulsed and CW Lasers
   S. D. Allen, Y.-C. Liu and A. B. Trigubo
   Optical Society of America
   Orlando, FL (10/81)

7. Properties of Several Types of Films Deposited by Laser CVD
   S. D. Allen and A. B. Trigubo
   American Vacuum Sociey
   Anaheim, CA (11/81)

* 8. Laser Surface Induced Chemistry
   Susan D. Allen
   Laser Institute of America
   Pasadena, CA (2/82)

* Invited

9. Laser CVD Using a CO_2 TEA Laser
S. D. Allen and Y.-C. Liu
Conference on Laser and Electro-Optics
Phoenix, AR (4/82)

* 10. Laser Chemical Vapor Deposition
Susan D. Allen
University of Arizona
Tucson, AR (4/82)

* 11. Laser Chemical Vapor Deposition Using CW and Pulsed Lasers
Susan D. Allen
SPIE
Washington, D.C. (5/82)

* 12. Laser Chemical Vapor Deposition - A New Thin Film Deposition Technique
Susan D. Allen
University of Wisconsin
Madison, WI (5/82)

* 13. Laser Chemical Vapor Deposition
Susan D. Allen
Naval Weapons Center
China Lake, CA (5/82)

14. Direct Writing Usin Laser Chemical Vapor Deposition
S. D. Allen, Y.-C. Liu, A. B. Trigubo and R. Y. Jan
Materials Research Society
Boston, MA (11/82)

* 15. Laser Chemical Vapor Deposition
Susan D. Allen
19th University Conference on Ceramic Science
Raleigh, NC (11/82)

* 16. The How and Why of Laser Deposition
Susan D. Allen
New Mexico American Vacuum Society Symposium
Albuquerque, NM (4/83)

* 17. Laser Activated CVD of Thin Films
Susan D. Allen
9th International Vacuum Congress and 5th International Conference on Solid Surfaces
Madrid, Spain (9/83)

* 18. Laser Chemical Vapor Deposition
Susan D. Allen
Materials Research Society
Boston, MA (11/83)

19. Chair
SPIE Symposium on Laser Deposition and Etching
Los Angeles, CA (1/84)

Laser chemical vapor deposition: A technique for selective area deposition

S.D. Allen
Center for Laser Studies, University of Southern California, University Park, Los Angeles, California 90007

(Received 5 May 1981; accepted for publication 17 July 1981)

Laser chemical vapor deposition (LCVD) uses a focused laser beam to locally heat the substrate and drive the CVD deposition reacton. Several different deposition reactions and substrates have been examined as a function of intensity and irradiation time using a CO_2 laser source: Ni on SiO_2, TiO_2 on SiO_2, TiC on SiO_2, and TiC on stainless steel. LCVD film thicknesses range from < 100 Å to $> 20\,\mu$m. Deposition rates of mm/min have been observed for LCVD Ni and $20\,\mu$m/min for LCVD TiO_2. The diameter of the deposited films is dependent on irradiation conditions and can be as small as one tenth of the laser beam diameter. The LCVD films exhibit excellent physical properties such as adherence, conductivity, hardness, and smoothness.

PACS numbers: 42.60.Kg, 81.15.Gh

INTRODUCTION

Chemical vapor deposition (CVD) is a technique for depositing coatings or growing layers on a substrate that is widely used in the semiconductor, optics, and refractory materials industries. In conventional CVD gaseous compounds which do not react at room temperature are passed over a substrate heated to a temperature at which either the reactants decompose or combine with other constituents to form a layer on the substrate. In this work the properties of several different types of films deposited by selective area CVD using a laser heat source are reported.

The use of a laser as the heat source for chemical vapor deposition offers several distinct advantages: (a) spatial resolution and control; (b) limited distortion of the substrate; (c) the possibility of cleaner films due to the small area heated; (d) availability of rapid, i.e., non-equilibrium, heating and cooling rates; and (e) the ability to interface easily with laser annealing and diffusion of semiconductor devices and laser processing of metals and alloys. It should be possible to generate deposits of almost any material that can be deposited by conventional CVD and probably some which cannot. Possible applications include: IC mask and circuit repair; writing interconnects for IC circuits; one-step ohmic contacts; localized protective coatings; localized coatings for waveguide optics; and localized wear and corrosion resistant coatings.

The deposition of material by thermal decomposition using a laser heat source was first reported for graphite from a hydrocarbon vapor in 1972[1] at the Third International Conference on Chemical Vapor Deposition. At the same conference the following year, D. M. Mattox[2] reported the LCVD of W by H_2 reduction of WF_6 using a multimode CW CO_2 laser translated across a SiO_2 substrate. More recently, the LCVD of polycrystalline Si from SiH_4 by Christensen and Lakin,[3] and CoO from cobalt acety acetonate and air by Steen[4] has been reported. In both cases, a CO_2 laser source and glass or quartz substrates were used.

I. EXPERIMENTAL PROCEDURE

Laser chemical vapor deposition (LCVD) is best described by referring to Fig. 1. The laser is focused through a transparent window and the transparent reactants onto an absorbing substrate, creating a localized hot spot at which the reaction takes place. The absorptivities of the reactants and the substrate determine the laser wavelength which is used.

Three different cases have been examined as a function of intensity and irradiation time using a CO_2 laser source: deposition of a reflecting film on a absorbing substrate, Ni-/SiO_2; an absorber on an absorbing substrate, TiO_2 and TiC-/SiO_2; and an absorber on a reflecting substrate, TiC/stainless steel.

Initial experiments on LCVD on SiO_2 substrates were carried out using the experimental apparatus illustrated in Fig. 2. The laser was a cw CO_2 rated nominally at 20 W, but usually run at about 10 W. Attenuation was provided by a ZnSe Brewster angle polarizer using two Brewster angle plates at opposing angles to minimize beam walkoff. Although the beam profile without the attenuator is approximately TEM_{00}, multiple reflections in the thin ZnSe plates introduce some distortion in the attenuated beam profile. The removable power meter and/or fluorescent viewing plates were used to check power stability and beam quality. Irradiation time was controlled by a mechanical shutter with

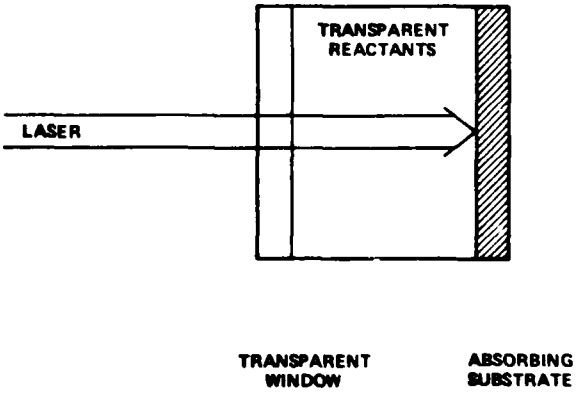

FIG. 1. Requirements for LCVD.

 0021-8979/81/116501-05$01.10

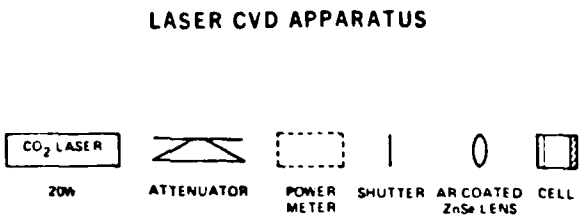

FIG. 2. Low-power LCVD apparatus.

speeds of 2.9 ms–1.0 sec. After the shutter, the beam was focused onto the absorbing substrate with a 10-in. focal length AR-coated ZnSe lens through a NaCl window. The reactions studied to date include:

$$Ni(CO)_4 \xrightarrow{140\,^{\circ}C} Ni + CO \quad \text{on quartz,}$$

$$TiCl_4 + H_2 + CO_2 \xrightarrow{900\,^{\circ}C} TiO_2 + HCl + CO \quad \text{on quartz,}$$

$$TiCl_4 + CH_4 \xrightarrow{1200\,^{\circ}C} TiC + HCl \quad \text{on quartz and stainless steel.}$$

The temperatures given for the reactions are the minimum deposition temperatures for the equilibrium CVD process.[5]

A. LCVD Ni

The deposition of Ni from $Ni(CO)_4$ is a well-known process and forms the basis for a purification technique for Ni, the Mond process.[6] The equilibrium kinetics of the CVD reaction have been studied by Carlton and Oxley,[7] who concluded that both heterogeneous and homogeneous reaction mechanisms contribute to the deposition. The absorption spectra of $Ni(CO)_4$ in the 9–11 μm range is dominated by a combination band at 920 cm^{-1} (Ref. 8) but at the pressure used (40 Torr) the absorption of a 1-cm pathlength at 10.6 μm (943 cm^{-1}) is less than 1%.

Two parameters of importance in evaluating LCVD are the resolution attainable, i.e., the minimum spot size, and the thickness of the deposit as a function of the irradiation conditions. For the LCVD of Ni on SiO_2 the spot diameter is

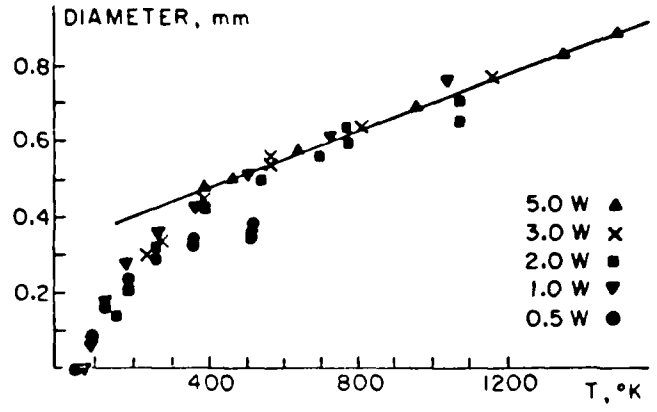

FIG. 4. Spot diameter (full width) of Ni films deposited on quartz ($T \propto It^{1/2}$). Laser beam diameter, $D_{1/e} = 0.6$ mm.

proportional to the square root of the irradiation time t, as shown in Fig. 3. If the spot diameter is plotted against the calculated surface temperature as in Fig. 4, the data for a wide range of deposition conditions (10X in power; 200X in irradiation time) lie on the same curve. For the range of spot sizes and irradiation times used, the surface temperature is proportional to $I_0 t^{1/2}$ (Refs. 9,10) where I_0 is the incident intensity and t is the irradiation time. From Fig. 4 it is apparent that there is an effective threshold for the deposition to occur. The diameter of the Ni spot increases rapidly above threshold but the rate of increase levels off for longer irradiation times and higher laser powers. This is particularly apparent for the $P_0 = 0.5$ W points. For incident powers higher than 0.5 W the deposited spot continued to grow for longer irradiation times, but at a slower rate. The spot diameters, in any case, are less than the diameter of the depositing laser beam, $D^2_{1/e} = 0.6$ mm, over most of the range of deposition conditions. This resolution enhancement can be understood by referring to Fig. 5. The surface temperature distribution is a Gaussian and the reaction occurs over that part of the Gaussian that is above the threshold temperature, effectively selecting the center of the Gaussian beam. Figure 6(a) is a profilimeter trace[11] of such a deposited spot illustrating the truncated Gaussian shape.

There is a change in the character of the deposition pro-

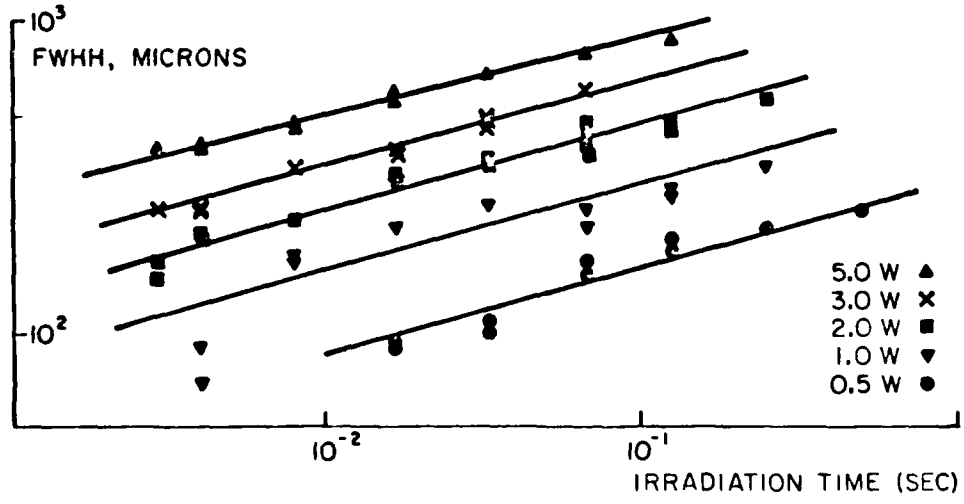

FIG. 3. Spot diameter (full-width at half height, FWHH) of Ni films deposited on quartz as a function of irradiation time. Laser beam diameter, $D_{1/e} = 600\,\mu$m.

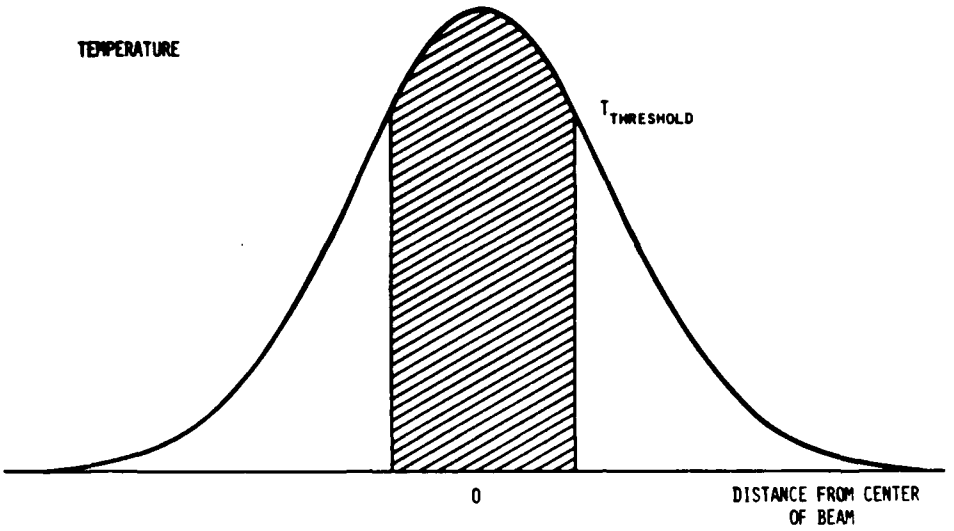

FIG. 5. Temperature distribution on a surface irradiated by a Gaussian laser beam.

file at the point in Fig. 4 where the curve becomes linear. A profilimeter trace[11] of such a spot is given in Fig. 6(b). Except for the 0.5 W points, all of the films produced in the linear region of Fig. 4 show this doubled-humped profile. The profilimeter traces, confirmed by SEM photographs, also show a roughened surface on the inside slopes of the "volcano" shape. Other parts of the deposited spot were essentially featureless (< 100 Å) while these areas had surface features on the order of 2000 Å in diameter. There are several possible explanations for these phenomena which are currently under investigation: (i) convection is beginning to play a role in the deposition rate, favoring the edge of the spot; (ii) the center of the spot becomes too hot and the sticking coefficient for the reactants decreases, favoring deposition in the cooler regions outside the center of the spot; (iii) at sufficiently high temperatures, carbon can be deposited by disproportionation of CO on the Ni surface and this might account for the observed nodules.

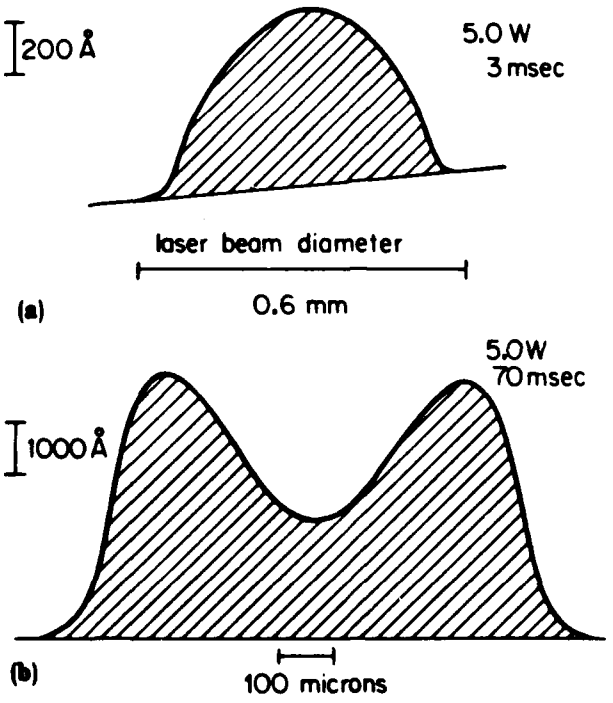

FIG. 6. Thickness profiles of LCVD Ni films.

The thickness of the deposited Ni films as a function of irradiation time t for various laser powers is given in Fig. 7. The functional dependence of the film thickness on irradiation parameters is more complex than in the case of the deposited spot diameter. The initial deposition rate is linear in t and varies from 1000 μm/min for incident power $P_0 = 5$ W, to 60 μm/min for $P_0 = 0.5$ W. The deposition rate at all incident laser powers decreases at a point corresponding to the onset of linear dependence in Fig. 4. At this same point, for incident powers greater than 1 W, the film profiles begin to show the doubled-humped "volcano" shape mentioned previously. The thickness plot for these data therefore splits into two curves when the profile shape changes; the upper curve corresponding to the maximum thickness and the lower to the thickness at the center of the deposited spot.

From a knowledge of the optical constants of quartz and Ni, one would predict that film thicknesses would be "self-limited" to approximately 200 Å using an optical heat source. The absorptivity of SiO_2 is approximately 0.9 at 10.6 μm (Ref.12) and the absorptivity of Ni is approximately 0.05.[13] One would therefore expect that once several hundred angstroms of metal were deposited on the substrate, the absorptivity of the surface would decrease by a factor of 18, the laser power absorbed, and the surface temperature would decrease correspondingly, and metal deposition would cease. This is obviously not the case as films of Ni on SiO_2 up to 1 μm in thickness have been deposited. Some evidence of thickness self-limiting is seen in the Ni deposition at low-incident laser powers, i.e., $P_0 = 0.5$ W, for long irradiation times. It is also observed in cases of multiple irradiation of a single site. The film thickness produced for n irradiations is less than $n \times$ the thickness for a single irradiation. A proper explanation of these results will require a knowledge of the deposition dynamics.

The hardness of LCVD Ni films was demonstrated by their resistance to scratching by a hardened steel pin. The

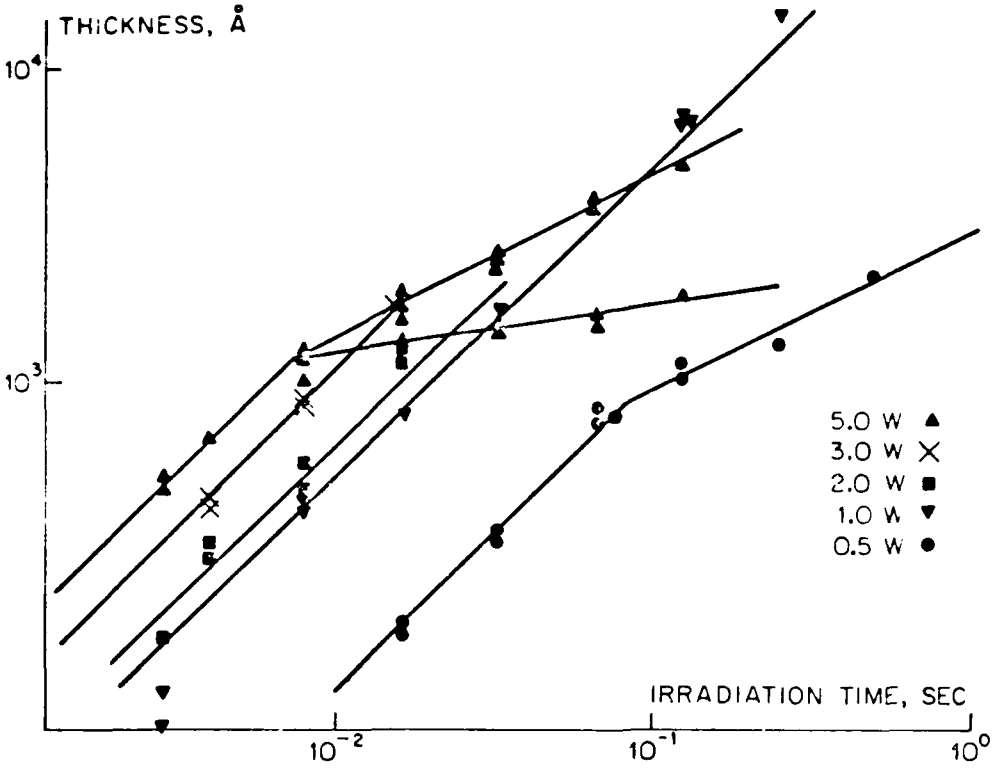

FIG. 7. Thickness of LCVD Ni films as a function of irradiation time. For the 5.0-W data the upper curve is the maximum thickness of the film, the lower curve is the thickness at the edge of the spot. Similar behavior is observed in the 3.0- and 2.0-W data but is not shown for reasons of clarity.

exceptions were those coatings deposited considerably above threshold, which were softer. The LCVD Ni films passed the Scotch tape adherence test with the same exception as in the hardness tests. Coatings produced by irradiation at high intensities for long times partially peeled when scrubbed with an alcohol-soaked cotton swab. The thickness of the LCVD Ni films ranged from 100 Å to 1 μm. The electrical conductivity was measured as less than $4\times10^{-5}\,\Omega$ cm for a 550-Å thick, large area film. Grain size, as measured by SEM, was less than 100 Å for most films. Nodules 2000 Å in diameter appeared on the inside slopes of the double-humped films deposited considerably above threshold.

B. LCVD TiO_2

The reaction for the TiO_2 deposition in the initial experiments belongs to a class known as "water-gas" reactions. In these reactions, H_2 and CO_2 combine at high temperatures to generate H_2O which reacts locally with an easily hydrolyzable compound, in this case, $TiCl_4$, to yield the product oxide. Deposition of oxide films by conventional CVD is difficult,[4] producing in many cases thin, pinhole-rich films with poor adherence.

$TiCl_4$ was vacuum-distilled into a side-arm tube of the deposition cell and 205 Torr each of CO_2 and H_2 added. The partial pressure of $TiCl_4$ was 12.4 Torr, the room-temperature vapor pressure. $TiCl_4$ is transparent at the CO_2-depositing laser wavelength.

The range of irradiation conditions over which TiO_2 can be deposited on quartz is narrower than that achieved with Ni/SiO_2, because the higher reaction temperature is close to the SiO_2 melting point. From the limited data available to date, the film thickness for LCVD TiO_2/SiO_2 is a linear or slightly greater than linear function of the irradiation time, similar to the near-threshold behavior of Ni/SiO_2 (Fig. 7). No evidence of self-limiting is observed or would be expected on the basis of the bulk optical constants. TiO_2 has a greater absorptivity than SiO_2 at 10.6 μm and multiple $n\times$ irradiations of the same site produced thicker films than would be predicted from $n\times$ (a single irradiation). Measured deposition rates range from 2–20 μm/min.

The resolution enhancement observed in the spot diameter of the Ni/SiO_2 system is also seen in the TiO_2/SiO_2 but no "volcano" thickness profiles were observed. The spatial profile could be tailored depending on irradiation conditions as shown in Fig. 8 from flat-topped to sharply peaked. These thickness profiles were measured using the interference colors observed in reflection microscopy and were checked by

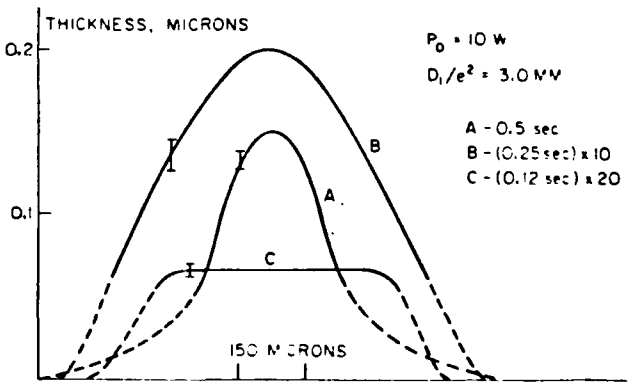

FIG. 8. Thickness profiles of LCVD TiO_2 films. (A) single irradiation of 0.5 sec, (B) 10 irradiations of 0.25 sec each, (C) 20 irradiations of 0.12 sec each.

stylus profilimetry.[11] For a single irradiation under conditions considerably above threshold the sharply peaked profile of Fig. 8(a) was observed. Multiple irradiation just barely above threshold produced the flat, uniform profile shown in Fig. 8(c). For deposition conditions lying between the two extremes, the broadly-peaked profile of Fig. 8(b) resulted. Various film thickness profiles are thus possible with a Gaussian laser intensity profile. This result is probably due to a combination of both diffusion and heat flow kinetics.

The TiO_2 films were clear and adherent. None was removed with vigorous scrubbing with an alcohol-soaked cotton swab. Preliminary results on the composition of the deposited films using scanning Auger microscopy (SAM) indicate that the composition, TiO_x, changes somewhat over the diameter of the larger deposited spots.

C. LCVD TiC

In conventional CVD of TiC (Ref. 5) the metal halide is combined with a hydrocarbon and H_2. For the LCVD experiments 220 Torr of CH_4 was added to a cell with a sidearm of vacuum distilled liquid $TiCl_4$. The presence of H_2 buffer gas is obviously not necessary for deposition of LCVD TiC as deposits up to 1-μm thick were formed on both steel and quartz substrates. The combination of a much lower absorptivity and a higher thermal conductivity means that the incident intensity necessary to achieve the deposition temperature for TiC is at least 10^2 greater on steel than on quartz. A Photon Sources 1.4-KW cw CO_2 laser was used for the steel deposition experiments. Coating thickness on steel substrates was measured by slant cutting the substrate and using SEM/EDAX to probe the Ti concentration across the depth of the coating. Stylus profilimetry was used to measure coating thickness on quartz and polished steel substrates.

The thickness of LCVD TiC on SiO_2 substrates shows a linear dependence on the irradiation time t similar to that observed for TiO_2 and near threshold for Ni on quartz substrates. No evidence of self-limiting was observed for the range of laser powers and irradiation times used. Multiple irradiations could be used to build up coating thickness on both quartz and steel with the rate of increase larger on the steel substrates. In several cases, multiple irradiations of a single site resulted in a melted area, indicating a greatly increased coupling efficiency of the laser into the substrate once a TiC layer had been deposited.

II. CONCLUSIONS

In conclusion, it has been demonstrated that LCVD can be used to deposit films of several different types of materials with area resolution equal to or better than the laser beam diameter. Reflective films deposited on absorbing substrates are not limited in thickness to several hundred Å by the changes in optical absorption as the films are deposited. In fact, Ni films several microns thick have been produced on quartz substrates. The cross-section shape of the deposited spot depends on reactants and irradiation conditions, varying from truncated Gaussian to flat-topped to a "volcano" shape. Physical properties of the deposited films are good to excellent. Other possible combinations of laser and substrate for LCVD include: visible lasers for semiconductor substrates, i.e., Si and GaAs, near UV lasers for glass substrates, and Nd:YAG lasers for metallic substrates.

ACKNOWLEDGMENTS

The author wishes to acknowledge the assistance furnished by Prof. A. Burg in the handling of $Ni(CO)_4$. This work was supported in part by a grant from AFOSR under the technical cognizance of H. Schlossberg.

[1]H. Lydtin, *Proceedings of the Third International Conference on Chemical Vapor Deposition*, edited by F. A. Glaski (Am. Nucl. Soc., Hinsdale, Illinois 1972), p. 121.
[2]R. S. Berg and D. M. Mattox, *Proceedings of the Fourth International Conference on Chemical Vapor Deposition*, edited by F. A. Glaski (Am. Nucl. Soc., Hindsdale, Illinois, 1973), p. 196.
[3]C. P. Christensen and K. M. Lakin, Appl. Phys. Lett. **32**, 254 (1978).
[4]W. M. Steen, Adv. in Surface Coating Tech., International Conference on Advances in Surface Coating Techniques, London, February, 1978.
[5]C. F. Powell, I. E. Campbell, and B. W. Gonser, *Vapor Plating* (Wiley, New York, 1955).
[6]L. Mond, Proc. R. Inst. G. B. **13**, 668 (1892).
[7]H. E. Carlton, and J. H. Oxley, AIChEJ **12**, 86 (1966).
[8]B. L. Crawford and P. C. Cross, J. Chem. Phys. **6**, 535 (1938).
[9]M. Sparks, J. Appl. Phys. **47**, 837 (1976); M. Sparks, and E. Loh, J. Opt. Soc. Am. **69**, 847 (1979).
[10]M. Lax, J. Appl. Phys. **48**, 3919 (1977); Appl. Phys. Lett., **33**, 786 (1978).
[11]Talystep Profilimeter measurements performed courtesy of J. Bennett, NWC, China Lake, California. Tencor profilimeter measurements courtesy of Griot Assoc., Los Angeles, California.
[12]D. E. Gray, *American Institute of Physics Handbook* (McGraw-Hill, New York, 1972).
[13]L. E. Howarth and W. G. Spitzer, J. Am. Ceram. Soc. **44**, 26 (1961).

Summary Abstract: Properties of several types of films deposited by laser CVD

S. D. Allen, A. B. Trigubo, and M. L. Teisinger

University of Southern California, Center for Laser Studies, University Park, Los Angeles, California 90007

(Received 20 November 1981; accepted 2 December 1981)

PACS numbers: 68.55. + b, 81.15.Gh, 79.20.Ds, 42.78.Hk

Films of TiO_2, GaAs, and TiC have been deposited by laser chemical vapor deposition (LCVD) on quartz and TiC deposited on steel using 20 and 1350 W cw CO_2 lasers, respectively. LCVD is an adaptation of conventional CVD using a laser heat source. The laser is focused through a transparent window and the transparent gaseous reactants onto an absorbing substrate, creating a localized hot spot at which the deposition reaction takes place. The optical absorptivities of the reactants and the substrate determine the laser wavelength which is used. Previous work in LCVD has emphasized deposition of atomic films such as W[1], Si[2], and Ni[3]. The compounds investigated in this work were chosen as representatives of materials for which selected area deposition would be desirable for optical coatings, hard coatings, and electronic applications.

The experimental apparatus used for deposition on quartz is shown in Fig. 1. The He–Ne beam collinear with the depositing CO_2 beam was used to monitor the deposition of the film in real time. The change in reflectivity for the CO_2 beam as the film was deposited was also monitored.

TiO_2 was deposited from $TiCl_4 + CO_2 + H_2$. $TiCl_4$ was vacuum distilled into a side-arm tube of the deposition cell and 205 T each of CO_2 and H_2 added. The partial pressure of $TiCl_4$ was 12.4 T, the room temperature vapor pressure. The irradiation conditions were: laser beam diameter $D_1/e^2 = 0.8$–3.0 mm; laser power $P = 5$–10 W; and irradiation time $t = 0.1$–1.0 s. The measured deposition rate was 300–3000 Å/s. The LCVD TiO_2 films were clear and adherent. Other properties are given in Ref. 3.

GaAs was deposited using the reaction: $Ga(CH_3)_3 + As(CH_3)_3 + H_2 \rightarrow GaAs + CH_4$. Both $Ga(CH_3)_3$ and $As(CH_3)_3$ were distilled into the side-arm of the deposition cell and 150 T of H_2 added. The side-arm of the cell was maintained at 0 °C and the vapor pressures of $Ga(CH_3)_3$ and $As(CH_3)_3$ were 65 and 98 T, respectively. The range of irradiation conditions over which deposition was observed was quite narrow: $D_1/e^2 \cong 0.6$ mm; $P_0 = 2$–3 W; and $t = 2$–12 s. For higher incident powers, deposition occurred in a ring around a center devoid of measurable GaAs. The surface temperatures achieved under these irradiation conditions are approximately the same as used for conventional MO CVD[4]: 600–900 °C.

The LCVD films were not continuous and showed a strong effect of nucleation sites on the substrate as shown in Fig. 2. The scratches on the surface of the substrate are readily apparent in the growth of the film. This type of deposition has been observed in conventional CVD on similar substrates.[5] Deposition rates were much slower than observed for other LCVD materials[3]: 150–500 Å/s, but were comparable to rates observed in conventional MOCVD.[4] Film thickness could be built up by multiple irradiations of the

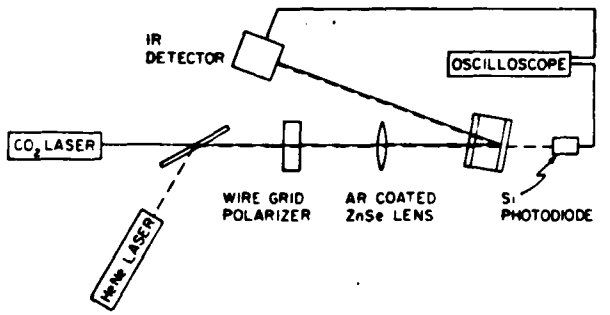

FIG. 1. Schematic diagram of the low power LCVD apparatus.

FIG. 2. SEM photograph of LCVD GaAs film (2 W, 11 s).

 0022-5355/82/030469-02$01.00

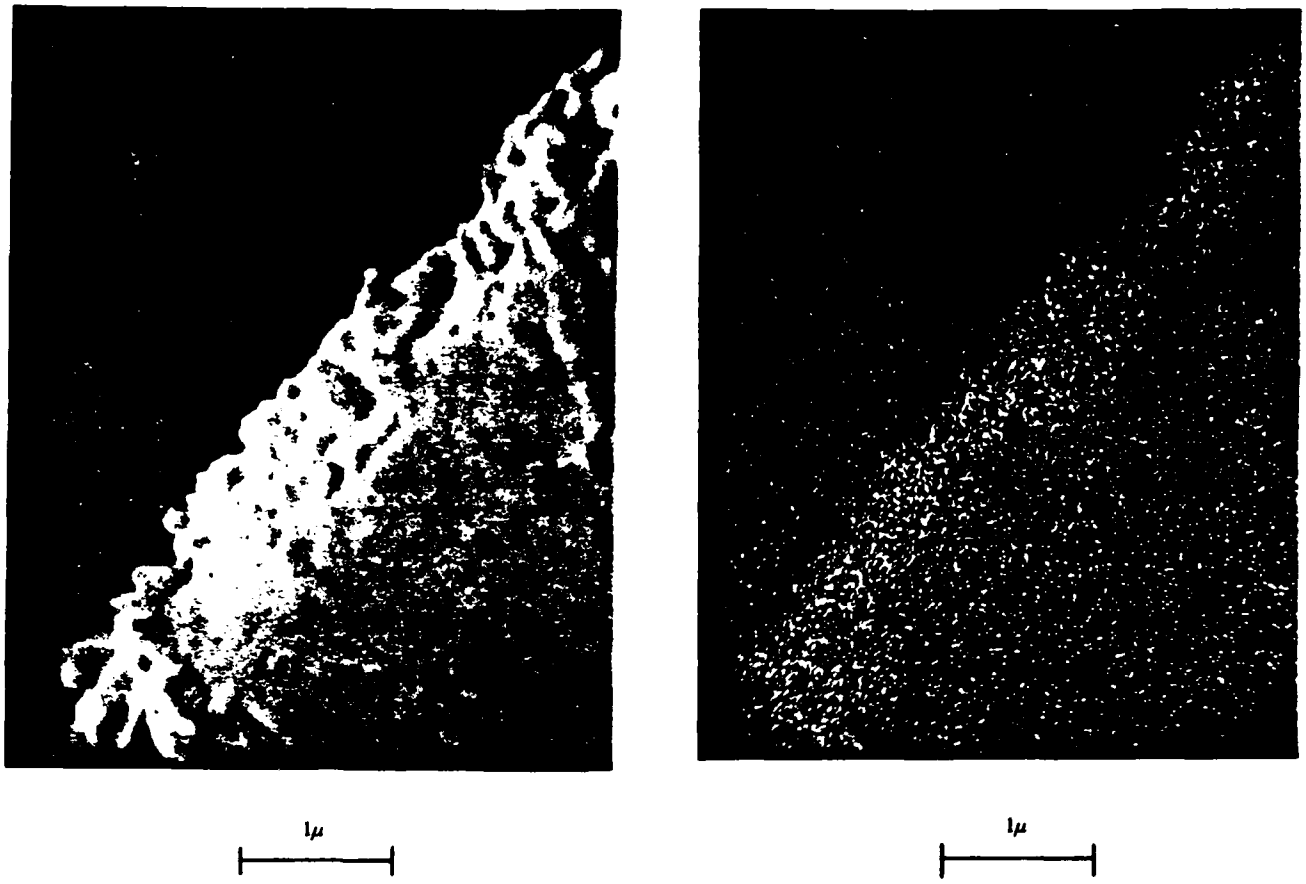

FIG. 3. (a) SEM photograph of fracture cross section of LCVD TiC film on carbon steel. (b) Ti x-ray map of the same area.

same site, resulting in films several microns thick and better but not complete coverage. In one case, the laser irradiated a site where some of the liquid material had condensed. The deposition rate observed was several orders of magnitude greater than in a "clean" site. The composition of the LCVD GaAs films was analyzed using SEM/EDAX. The Ga/As ratio varied with irradiation conditions from 0.3 to 2.0, bracketing the value for pure GaAs, 0.73.

In order to deposit TiC on carbon steel substrates, several orders of magnitude more laser power is necessary due to the decreased absorptivity and increased thermal diffusivity of the steel relative to quartz. TiC was deposited from $TiCl_4$ at the room temperature vapor pressure of 12 T and CH_4 or C_2H_2 (200 T) with and without H_2 (200 T). The high power LCVD apparatus consisted of a stainless steel tank electroless Ni plated with x and y translation stages driven by an external stepping motor. Coating tracks were deposited by translating the substrate under the stationary CO_2 laser beam. Incident powers were 500–1200 W, $D_f/e^2 = 1$–2 mm and translation speeds of 3–6 mm/s.

A SEM of the fracture cross section of a typical LCVD TiC track is given in Fig. 3(a) along with the Ti x-ray map of the same area [Fig. 3(b)]. The Ti is concentrated in the fine grained region shown in Fig. 3(a) which corresponds to the LCVD TiC coating. The fine grained material has a grain size of 500–1000 Å. These LCVD tracks show increased surface hardness but are not thick enough (typically 0.5–1.0 μ) for the hardness to be measured directly.

In conclusion, several different types of compound films have been deposited using LCVD. The results are promising but the deposition conditions have not been optimized and further work is necessary.

[1]R. S. Berg and D. M. Mattox, in *Proceedings of the Fourth International Conference on Chemical Vapor Deposition*, edited by F. A. Glaski (Amer. Nuclear Soc., Hinsdale, Ill., 1973), p. 196.
[2]C. P. Christensen and K. M. Lakin, Appl. Phys. Lett. 32, 254 (1978).
[3]S. D. Allen, J. Appl. Phys. 52, 6501 (1981).
[4]P. D. Dapkus, H. M. Manasevit, and K. L. Hess, J. Cryst. Growth 55, 10 (1981).
[5]P. D. Dapkus (private communication).

Laser chemical vapor deposition of selected area Fe and W films[a)]

S. D. Allen and A. B. Tringubo
Center for Laser Studies, University of Southern California, Los Angeles, California 90089-1112

(Received 2 September 1982; accepted for publication 2 November 1982)

Localized deposition of thin films of W and Fe in both spot and line geometries has been demonstrated by laser chemical vapor deposition using a CO_2 laser and several different gaseous reactants. Although optical self-limiting of the deposit thickness was observed under some irradiation conditions, films several thousand Å thick could be deposited with good physical properties. Radial dimensions were less than or equal to the laser beam diameter ($D_{1/e^2} = 600$ μm).

PACS numbers: 81.15.Gh, 78.65.Ez, 73.60.Dt

High-resolution pattern generation for both IC's and printed wiring is normally accomplished with multistep photoresist techniques. There are some applications, however, where additive photoresist processing is very difficult or impossible, e.g., repair of IC's and the photomask itself; tuning and trimming of circuit elements that require addition of material; custom design; and large-area depositions on nonflat surfaces such as interconnects on large Si wafers and high-resolution printed wiring. In these and similar situations, a method of direct or maskless pattern generation is desirable. Laser chemical vapor deposition (LCVD) is one of several recently developed techniques utilizing a laser to effect localized deposition.[1-4] For LCVD[1] and other thermally driven laser deposition,[2] the laser wavelength is chosen such that reactants are transparent and the substrate absorbing. Focusing the laser through the gaseous reactants onto the substrate creates a localized hot spot at which the deposition takes place.

LCVD of metals, insulators, and semiconductors has previously been reported.[1,5] For the LCVD of Ni from $Ni(CO)_4$ on quartz substrates using a cw CO_2 laser,[1] it was found that the deposition rate was a constant with irradiation time for a constant-intensity laser pulse. This behavior is not what would be expected for deposition using an optical heat source. For the case of a reflecting (i.e., metal) film deposited on a highly absorbing substrate, the absorbed laser intensity, and therefore the substrate temperature, decreases as the film is deposited. As a result, the deposition rate should also decrease. We report here the LCVD of Fe and W films, and the observation of optical self-limiting of the film thickness for some irradiation conditions.

LCVD depositions were carried out using both the apparatus previously described[1] and a modification described below. The new apparatus utilizes an electrically pulsed, tunable cw CO_2 laser with maximum output power of 40 W. Attenuation of the beam was provided by a wire-grid polarizer. A removable power meter and/or fluorescent viewing plates were used to check power stability and beam quality. The beam was focused through a NaCl window onto the absorbing substrate with a 10-in.-focal-length AR-coated ZnSe lens. The beam profile at the substrate was approximately gaussian with a $D_{1/e^2} \simeq 600$ μm. The temporal intensity profile of pulses 1 ms or longer was approximately a step function with some initial overshoot, as measured using a HgCdTe detector. The reactions studied include

$$WF_6 + H_2 \xrightarrow{600\,^\circ C} W + HF;$$

$$W(CO)_6 \xrightarrow{350\,^\circ C} W + CO;$$

$$Fe(CO)_5 \xrightarrow{370\,^\circ C} Fe + CO.$$

The temperatures given for the reactions are the minimum reacommended deposition temperatures for the conventional CVD process.[6] Because the amount of reactant used during LCVD is a small fraction of the total concentration, the depositions were carried out with closed reaction cells.

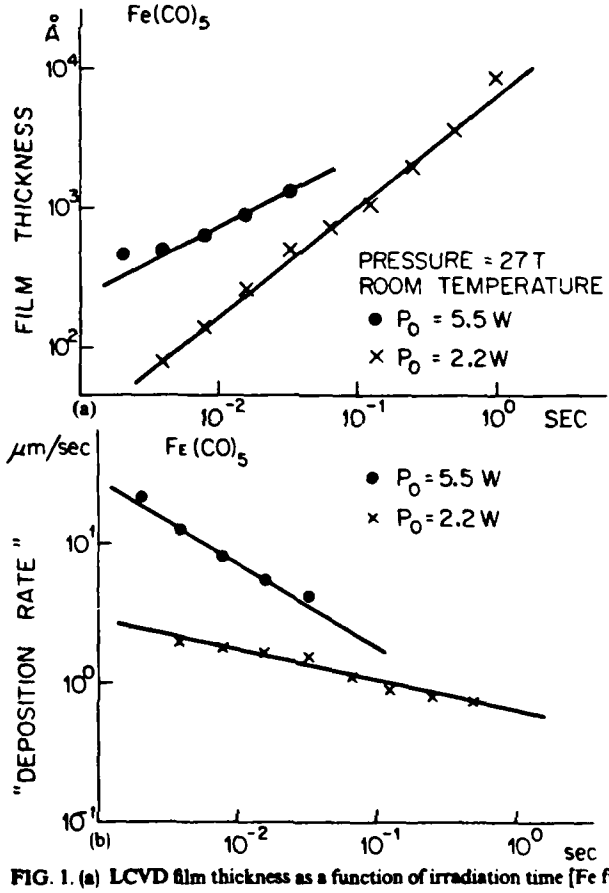

FIG. 1. (a) LCVD film thickness as a function of irradiation time [Fe from $Fe(CO)_5$]. (b) Apparent deposition rate (film thickness/irradiation time) as a function of irradiation time [Fe from $Fe(CO)_5$].

[a)]Supported in part by Air Force Office of Scientific Research Grant No. AFOSR 79-0135.

 0021-8979/83/031641-03$02.40

$Fe(CO)_5$, a liquid at room temperature, was vacuum distilled into a side arm of the deposition cell using a vacuum system with a base pressure of 5×10^{-6} Torr. Care was taken to avoid illumination of the cell with fluorescent light in order to suppress the photochemical formation of $Fe_2(CO)_9$.[7] The deposition wavelength of 10.6 μm was chosen because it lies at an absorption minimum in the spectra of $Fe(CO)_5$.[7,8] The room-temperature vapor pressure of 27 Torr was used for all deposition measurements.[9]

The thickness of the LCVD Fe films as a function of irradiation time τ for several laser powers is given in Fig. 1(a). For irradiation times longer than the maximum given for each case, the deposition thickness profiles deviated significantly from the truncated gaussian shape observed[1] for short irradiation times. In contrast to the similar data for Ni,[1] the thickness is not a linear function of the irradiation time, and the lower intensity data (2.2 W) exhibits a steeper slope (thickness proportional to $\tau^{0.8}$) than the higher intensity points (5.5 W, thickness proportional to $\tau^{0.5}$). The same data is replotted in Fig. 1(b) as the apparent deposition rate, defined as the deposit thickness divided by the irradiation time. The actual deposition rate is a more complicated function of the heating time and the changing absorptivity of the surface during deposition, but this definition serves to illustrate qualitatively the optical self-limiting of the film thickness. For the shortest irradiation times, 2 ms, the higher incident laser intensity yields a faster deposition rate, in accord with the higher laser-generated surface temperature. As the irradiation time increases, however, the deposited film reflects increasing amounts of the incident energy and the surface temperature decreases. The deposition rate should therefore approach a constant for long irradiation times. Before this point, however, other limiting mechanisms come into play. For example, diffusion processes may lead to a decreased reactant concentration at the center of the laser-heated spot for relatively long irradiation times, resulting in decreased deposition at the spot center. This phenomenon has been observed as changes in the LCVD film thickness profile from truncated gaussian to flat-topped to a volcano shape with increasing irradiation time for most systems observed.[1]

Another indication that optical self-limiting is occurring is given by the data of Fig. 2. Multiple irradiations of 3 ms each at 5.5 W incident power were made on a single site. After the initial deposition of approximately 500 Å, no additional deposition is observed. For the multiple depositions, the site is allowed to cool to ambient between each irradiation, and change in reflectivity from the uncoated quartz ($R = 0.10$) to several hundred Å of Fe ($R = 0.94$)[10] would decrease the laser-generated surface temperature by almost an order of magnitude. For the continuously irradiated site, the decrease in surface absorptivity occurs on an already heated substrate, and the surface temperature decreases, but may remain above the deposition temperature.

The deposited spots and lines were adherent, hard, shiny, and metallic looking. Surface microstructure was similar to Ni deposited from $Ni(CO)_4$,[1] and was essentially featureless to less than the resolution of the scanning electron microscope (100 Å). Resistivity measurements on lines generated by translating the substrate under the laser beam,

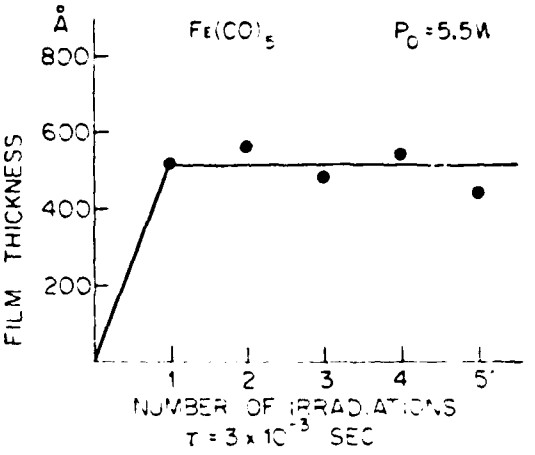

FIG. 2. LCVD film thickness for multiple irradiated sites [Fe from $Fe(CO)_5$].

however, showed very high resistivities which increased with time, implying heavy oxidation of the thin (250 Å) lines. Optimization of scan speed should produce thicker deposits which would minimize the effects of oxidation. Single-site irradiation has produced films 1 μm thick.

LCVD of W from $WF_6 + H_2$ was carried out as a function of irradiation conditions for WF_6 pressures ranging from 40 to 200 Torr with a constant H_2 pressure of 400 Torr. The deposition wavelength lies on the shoulder of an absorption band,[11] but the total absorption for the pressures used was 5% or less. The apparent deposition rate is plotted in Fig. 3 as a function of the irradiation time. In this case, the deposition was carried out with the same laser intensity, but with different concentrations of WF_6. The higher concentrations of WF_6 yielded greater initial deposition rates, as expected from kinetic considerations, which decreased faster with increasing irradiation time. For irradiation times on the order of 1 s, the apparent deposition rate is the same for both reactant concentrations. (The lower pressure data for times greater than 1 s is spuriously high because of buckling of the

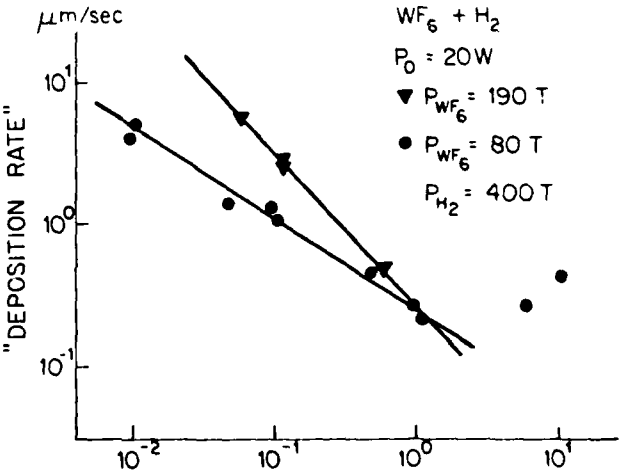

FIG. 3. Apparent deposition rate (film thickness/irradiation time) as a function of irradiation time (W from $WF_6 + H_2$).

W films.) This functional behavior is consistent with the optical self-limiting mechanism.

Lines were again generated by translating the substrate under the laser beam at speeds of 1–10 cm/s. Cross-sectional profiles were approximately trapezoidal with widths varying from 150 to 400 μm depending on scan speed and incident intensity. Resistivity measurements of lines 0.5 cm long, 600 Å thick, and 400 μm wide and 0.5 cm long, 1500 Å thick, and 160 μm wide yielded 2×10^{-5} and 6×10^{-5} ohm cm, respectively. These numbers compare favorable to the bulk resistivity of W, $\rho = 6\times10^{-6}$ ohm cm,[10] particularly since the LCVD conditions have not been optimized. With the exception of irradiation times much greater than 1 s, the LCVD films were quite adherent. Scanning electron microscope examination of the LCVD films revealed surface structure that varied from smooth (no observable features greater than 100 Å), to grandular nodules approximately 1000 Å in diameter, to small crystallites approximately 3000 Å in diameter. This change in surface structure appears to be related to both irradiation conditions and diffusion processes.

Only preliminary data has been obtained on LCVD W from $W(CO)_6$ because of several complications. A solid at room temperature, $W(CO)_6$ has a vapor pressure of less than 0.1 Torr at 30 °C.[8] The deposition rate observed for such a low concentration was very low, requiring several seconds to deposit a visible metallic film. At the higher pressures obtained with a heated deposition cell ($P = 20$ Torr at 105 °C), there is significant absorption of the 10.6-μm wavelength.[12] Experiments at other wavelengths are in progress.

In conclusion, we have shown that for a constant intensity laser pulse, the change in absorptivity of the substrate/film combination can lead to self-limiting of the film thickness for some materials. The effect is more pronounced for reactions occurring at higher temperatures and was not observed for the very low temperature reaction, $Ni(CO)_4 \rightarrow Ni + CO$.[1] In this case, the surface temperature of the substrate after the deposition of a thin film of Ni is still above the minimum deposition temperature. Initial deposition rates on the order of 10 μm/s were oberved, and films several thousand Å thick could be deposited. In order to generate thicker films of these materials, the laser power should be increased to compensate for the decreased absorptivity of the substrate. Experiments to monitor the reflected infrared beam intensity with the goal of real-time control of the incident laser power are in progress. Spot diameters varied from 150 to 600 μm (0.25 to 1 times the laser beam diameter), and spot diameters on the order of 1 μm should be attainable with shorter wavelength lasers. Physical properties of the LCVD films are good to excellent when deposited under the proper irradiation conditions.

[1] S. D. Allen, J. Appl. Phys. **52**, 6501 (1981).
[2] J. Cl. Puippe, R. E. Acosta, and R. J. von Gutfeld, J. Electrochem. Soc. **128**, 2539 (1981).
[3] D. J. Ehrlich, R. M. Osgood, Jr., and T. F. Deutsch, IEEE J. Quantum Electron. **QE-16**, 1233 (1980).
[4] V. Baranauskas, C. I. Z. Mammana, R. E. Klinger, and J. E. Greene, Appl. Phys. Lett. **36**, 930 (1980).
[5] S. D. Allen, A. B. Trigubo, and M. L. Teisinger, J. Vac. Sci. Technol. **20**, 469 (1982).
[6] C. F. Powell, J. H. Oxley and J. M. Blocker, Jr., *Vapor Deposition* (Wiley, New York, 1966).
[7] R. K. Sheline and K. S. Pitzer, J. Am. Chem. Soc. **72**, 1107 (1950).
[8] W. F. Edgell, W. E. Wilson, and R. Summitt, Spectrochim. Acta **19**, 863 (1963).
[9] *Organic Synthesis Via Metal Carboyls*, edited by I. Winder and P. Pino (Wiley, New York, 1968).
[10] *American Institute of Physics Handbook*, edited by D. E. Gray (McGraw-Hill, New York, 1972).
[11] T. G. Burke, D. F. Smith, and A. H. Nielsen, J. Chem. Phys. **20**, 447 (1952).
[12] L. H. Jones, Spectrochim. Acta **19**, 329 (1963).

S. D. ALLEN, A. B. TRIGUBO, AND R. Y. JAN
Center for Laser Studies, University of Southern California, University Park
DRB 17, Los Angeles, California 90089-1112 USA

ABSTRACT

Metal, dielectric and semiconductor films have been deposited by laser chemical vapor deposition (LCVD) using both pulsed and cw laser sources on a variety of substrates. For LCVD on substrates such as quartz, the deposition was monitored optically in both transmission and reflection using a collinear visible laser and the depositing CO_2 laser. Deposition initiation and rate were correlated with irradiation conditions, the laser generated surface temperature, and the changing optical properties of the film/substrate during deposition. Single crystallites of W greater than 100 μm tall were deposited using a Kr laser on Si substrates.

INTRODUCTION

Laser chemical vapor deposition (LCVD) is one of several recently developed laser deposition techniques [1]. The goals of these new methods are predominantly twofold: 1) maskless pattern generation by direct laser writing and 2) deposition of materials with novel properties such as controlled structure and grain size, increased adherence, modified electrical properties, and enhanced deposition at low temperatures. These effects can be achieved by localizing the heated area in the thermal processes and by absorbing the laser energy directly into the reactive species in the photochemical processes.

LCVD is an adaptation of conventional CVD using a laser heat source. The laser is focused through a transparent window and the transparent gaseous reactants onto an absorbing substrate, creating a localized hot spot at which the deposition reaction takes place. Although the process is thermal, it can be employed for deposition on heat sensitive structures because the heating is localized. The very rapid deposition rates (>100 μm/sec) achievable with LCVD, in combination with fast laser heating rates (~ 10^{10} °C/sec) should allow the deposition of very small area (≤1 μm diameter) coatings with a minimum heat affected zone in the substrate. Modification of structural and electrical properties can be achieved by control of the laser heated surface temperature, growth rate, dopants, and post growth annealing. Metal [2,3], semiconductor [4], and dielectric [3,4] films have been deposited by LCVD on a variety of substrates using both pulsed and cw lasers in this laboratory. In this paper we will discuss the LCVD of metal films on quartz and Si substrates using CO_2 and Kr lasers.

For the deposition of a reflecting (i.e., metal) film on a highly absorbing substrate using a constant intensity optical heat source, it would be expected that the film would be optically self-limited to a thickness on the order of

the optical absorption depth or several hundred Å. As the film is deposited the absorbed laser intensity decreases and therefore the substrate temperature and the deposition rate decrease. A comparison of the optical constants of most metals and quartz at 10.6 μm shows that the absorptivity changes by approximately an order of magnitude once several hundred Å of metal are deposited and the surface temperature should decrease accordingly. The LCVD process, in this case, can be characterized by an initial surface temperature rise to near the deposition temperature, a decrease in the surface temperature as the film is deposited, and, finally, attainment of an equilibrium temperature which may or may not be above the minimum deposition temperature. The effective deposition rate, defined as the deposit thickness divided by the irradiation time, is thus a complicated function of not only the irradiation conditions and the reaction kinetics but also the optical constants of both the substrate and the LCVD film.

EXPERIMENTAL

LCVD Ni, Fe, W/SiO_2

For the LCVD of W from $WF_6 + H_2$ on quartz substrates using a CO_2 laser, the expected optical self-limiting does occur, with the deposited film thickness under most conditions independent of the irradiation time with a maximum film thickness is 2500 - 5000 Å depending on irradiation conditions and reactant concentration. At the other extreme, the LCVD rate for Ni from $Ni(CO)_4$ is linear with irradiation time up to a film thickness of several thousand Å for a range of incident intensities. LCVD Fe from $Fe(CO)_5$ is an intermediate case with the film thickness, l, proportional to the irradiation time, $\tau^{0.8}$, for an incident power of 2.2 W and to $\tau^{0.5}$ for an incident power of 5.5 W [3].

In order to understand this behavior, optical monitoring of the LCVD film deposition was undertaken with the apparatus shown in Fig. 1. The laser is an electrically pulsed, line tunable cw CO_2 with maximum output power of 40 W.

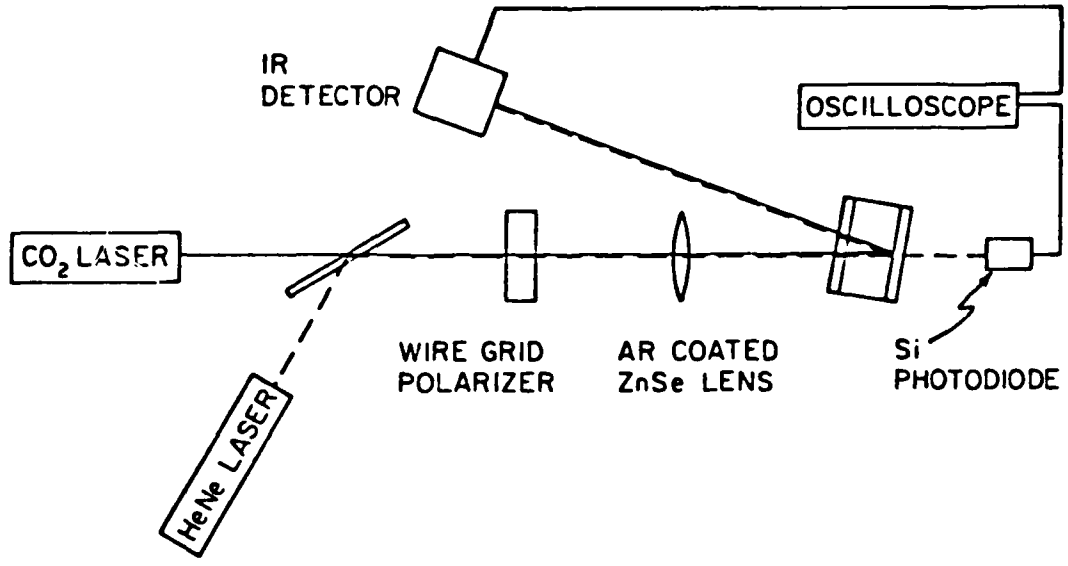

Fig. 1. Schematic diagram of the LCVD apparatus.

TABLE 1
Relative and calculated surface temperature for different irradiation conditions (W from $WF_6 + H_2$)

P (W)	τ (msec)	$P\tau^{\frac{1}{2}} \alpha T_s$ ($W\ msec^{\frac{1}{2}}$)	T_s (calc) (^oC)
4.7	55.8	35.1	810
7.0	22.5	33.2	880
10.0	10.9	33.0	950
15.0	4.9	33.2	990

assumptions, however. For quartz it is necessary to take into account the temperature dependence of the thermal properties such as heat capacity and thermal diffusivity. The formalism developed for the calculation of the laser heated surface temperature for Si [7,8] cannot be used for quartz because of the large differences in the thermal properties of the two materials. Iterative calculations using the measured thermal properties of fused quartz [9] yield the temperature vs. irradiation time curves given in Figure 3 for incident intensities corresponding to the experimental conditions of Table 1. The on-axis surface temperatures calculated for the irradiation times at which deposition begins are also given in Table 1. The calculated temperatures are not constant, but the range of values is small and falls well within the optimum temperatures used in conventional CVD for this system [10].

In terms of the model of LCVD discussed previously in which the process could be described by an initial heating period, deposition initiation, surface temperature decrease for deposition of a metal on an absorbing substrate, and attainment of an equilibrium surface temperature, the difference in effective deposition rate measured for Ni, Fe, and W is predominantly due to the large differences in the threshold deposition temperatures for the reactions. The Ni from $Ni(CO)_4$ deposition occurs at a very low temperature (~100°C, Ref. [10]) and for the irradiation conditions chosen for LCVD Ni, the equilibrium surface temperature is greater than this deposition temperature. A deposition rate which is constant with increasing irradiation time would therefore be expected once the LCVD film thickness exceeded several hundred Å. For W from $WF_6 + H_2$, the deposition temperature is almost an order of magnitude larger [10] and the equilibrium temperature calculated using the W optical constants is less than the deposition temperature and severe optical self-limiting occurs. The deposition temperature for Fe from $Fe(CO)_5$ is an intermediate case and the observed optical self-limiting is less severe than for LCVD W.

The LCVD Ni, Fe, and W deposits were hard, shiny, and metallic. Adherence was good for the Ni and Fe coatings up to a thickness of approximately 1 μm. LCVD W coatings greater than about 3000 Å thick also showed some indication of peeling. Resistivity measurements of Ni and W films 500 - 1500 Å thick in both sheet and line geometries yielded values of 3-10 times the bulk

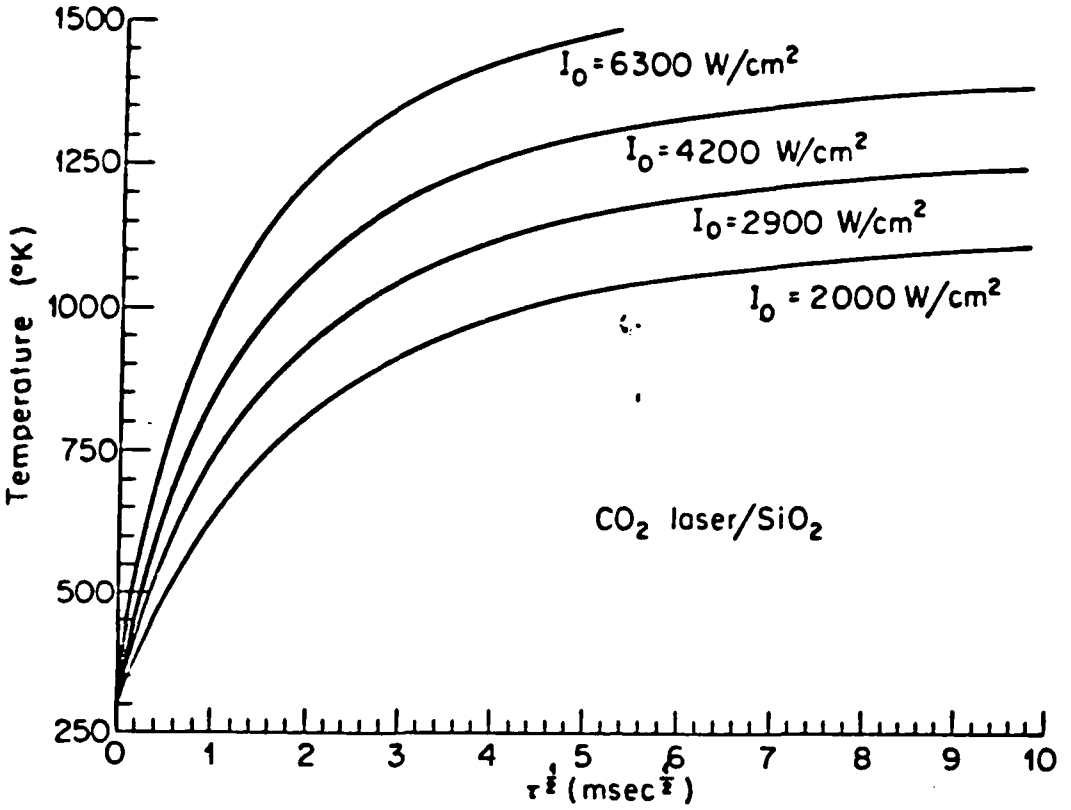

Fig. 3. Calculated surface temperature for fused quartz as a function of irradiation time for several incident laser intensities.

resistivities of the pure metal. These values of the resistivity are quite good for thin films deposited under unoptimized conditions. The lines were drawn by translating the substrate relative to the laser beam. The LCVD Ni and Fe films examined by scanning electron microscopy (SEM) revealed no surface microstructure to less than the resolution of the instrument (100 Å). LCVD W films varied from essentially featureless to a surface nodular structure (diameter approximately 2000 Å) to small crystallites (approximately 4000 Å) depending on irradiation conditions.

LCVD W/Si

An apparatus similar to Figure 1 but without the He-Ne optical monitoring was used to deposit W from WF_6 (200 T) + H_2 (400 T) on Si substrates using a Kr laser. The blue-green (468 - 530 nm) lines of the Kr laser are strongly absorbed by the Si and most gaseous reactants are transparent in the visible, satisfying the LCVD requirements. The laser is focused with a 6.5 cm focal length lens onto the substrate yielding a beam diameter of approximately 20 μm at the focus. The intensity profile deviates considerably from TEM_{00}, having a large TEM_{01*} component. Lines and spots were deposited at scan speeds of 0.2 - 2.0 mm/sec at laser powers of 3 - 4 W. For the slower speeds and higher incident powers, melting of the substrate was observed. Because the absorptivities of the Si and the W are similar in this wavelength region, it was possible to deposit thicker lines than could be achieved on fused quartz substrates. Multiple irradiations could also be used to build up deposit thickness. Unfortunately, these thicker lines (l = several microns) peeled when the substrate was stressed during removal from the mount.

A curious growth pattern was observed for some spot depositions. Single crystal W spikes (Figure 4) could be deposited with dimensions on the order of 40 - 50 μm wide and 50 - 120 μm tall. These are similar in geometry to the polycrystalline C and Si rods deposited by LCVD by Bauerle et. al., [11,12], but the appearance of one or at most a few large crystals has not previously

Fig. 4. SEM of LCVD W deposited on a Si substrate using a Kr laser.

been observed. The growth rates measured for these crystallites approach a mm/sec. Such structures have not been observed for LCVD W on SiO_2 using the CO_2 laser for similar reactant concentrations. It appears that the difference in growth habit is related to the large difference in the laser heated areas in the two cases. Examination of a LCVD W spot on Si (Figure 5) where single crystal growth did not take place reveals the familiar "volcano" shape observed in LCVD with the CO_2/SiO_2 system [2]. In the center of the volcano are small crystallites which are miniature versions of the large single crystal of Figure 4. Because the Kr laser irradiates an area on the order of 10 μm as opposed to the hundreds of microns irradiated by the CO_2 laser, it is possible for one or several of these crystallites to dominate the growth. LCVD W spikes have been deposited with 1 - 4 crystallites apparent in the SEM photographs.

CONCLUSIONS

Metal films with good physical properties have been depsoited by LCVD on fused quartz and Si substrates at scan speeds of cm/sec and deposition rates approaching mm/sec. Using UV laser sources it is possible to achieve deposit geometries on the order of 1 - 2 μm with good prospects for further reduction of dimensions [13,14]. LCVD is thus an excellent candidate process for direct writing of metal patterns for microelectronics and other applications. LCVD film growth initiation and deposition rate for the CO_2/SiO_2 system have

Fig. 5. SEM of LCVD W deposited on a Si substrate using a Kr laser.

been monitored optically and the deposition initiation can be explained qualitatively using a simple threshold temperature model and laser heated surface temperature calculations which include temperature dependent thermal properties of the quartz substrate. LCVD of single crystal rods greater than 100 μm tall of W on Si substrates has been observed.

ACKNOWLEDGMENTS

This work was supported in part by a grant from AFOSR under the technical administration of H. Schlossberg.

REFERENCES

1. See, for example, other papers in these proceedings.

2. S. D. Allen, J. Appl. Phys. 52, 6501 (1981).

3. S. D. Allen and A. B. Trigubo, J. Appl. Phys., to be published (2/83).

4. S. D. Allen, A. B. Trigubo, and M. L. Teisinger, J. Vac. Sci. Tech. 20, 469 (1982).

5. W. W. Duley, CO_2 Lasers: Effects and Applications (Academic Press, New York, 1976).

6. J. F. Ready, Effects of High-Power Laser Radiation (Academic Press, New York, 1971).

7. Y. I. Nissim, A. Lietoila, R. B. Gold, and J. F. Gibbons, J. Appl. Phys. 51, 274 (1980).

8. J. E. Moody and R. H. Hendel, J. Appl. Phys. 53, 4364 (1982).

9. A. Goldsmith, T. E. Waterman, and H. J. Hirschhorn, Handbook of Thermophysical Properties of Solid Materials (Macmillan, New York, 1961).

10. C. F. Powell, J. H. Oxley, and J. M. Blocher, Jr., Vapor Deposition (Wiley, New York, 1966).

11. G. Leyendecker, D. Bauerle, P. Geittner and H. Lydtin, Appl. Phys. Lett. 39, 921 (1981).

12. D. Bauerle, P. Irsigler, G. Leyendecker, H. Noll, and D. Wagner, Appl. Phys. Lett. 40, 819 (1982).

13. G. Tisone and A. W. Johnson, private communication.

14. D. Ehrlich, R. M. Osgood, Jr., and T. F. Deutsch, Amer. Vac. Soc. Meeting, Nov. 1981.

Ceramic Conference held Nov. '82 at North Carolina State University

LASER CHEMICAL VAPOR DEPOSITION (LCVD)

Susan D. Allen

Center for Laser Studies
University of Southern California
Los Angeles, CA 90089-1112

INTRODUCTION

Laser chemical vapor deposition (LCVD) is one of several recently developed deposition techniques using laser sources. The two predominant characteristics of a laser light source - its directionality and its monochromaticity - can both be used to advantage in the deposition of materials. The directionality inherent in a laser source allows energy to be aimed very precisely at an area with dimensions on the order of the wavelength of the particular laser, causing localized deposition. The monochromaticity can be used to deposit energy directly into reacting molecules by exciting either electronic or vibrational energy levels in the reacting species. This precise control of energy flow in the system allows the deposition to occur at substrate temperatures much below those required for thermal equilibrium.

The several kinds of laser deposition can be conveniently divided into two types: thermal and photochemical. A generalized laser deposition experimental arrangement is given in Fig. 1. For thermally driven laser deposition such as LCVD [1-8] and laser enhanced electroplating (LEEP) [9] the laser wavelength is chosen such that the reactants are transparent and the substrate absorbent. Focusing the laser on the substrate creates a localized hot spot at which the deposition takes place. For laser photochemical deposition (LPD) [10-15] the reverse conditions apply - the laser is absorbed by the reactants and the substrate is transparent. The focused laser creates a high concentration of reactive species near the substrate, causing localized deposition. In an alternative geometry, large areas can be coated using LPD by directing

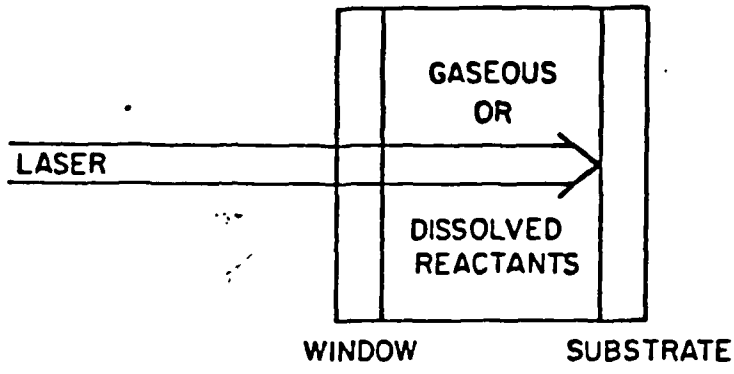

Fig. 1. Generalized laser deposition experimental arrangement.

the laser parallel to the substrate. Many of these techniques can also be utilized in reverse, i.e., to cause localized or low temperature etching. Table 1 gives the range of experimental conditions and the materials deposited for three types of laser deposition. Other variations of both thermal and photochemical laser deposition are, of course, possible, e.g., photoelectrochemical deposition [17] and LCVD from solution on semiconductor substrates [18]. The advantages of laser deposition are, in general, those associated with other laser processing techniques: a) spatial resolution and control; b) availability of rapid, nonequilibrium deposition conditions; c) localization of heating in the thermal processing or low temperature processing in LPD; d) increased purity of the deposits; and e) ability to interface easily with other laser processing techniques such as laser annealing and contact formation in semiconductors and laser processing of metals and ceramics.

EXPERIMENTAL

In this laboratory we have investigated a wide range of LCVD reactions (Table 2) on metallic, semiconductor and insulator substrates using pulsed and cw infrared and visible lasers. Not all of the reactions given in Table 2 yielded good results under the conditions used in the preliminary survey. For example, the LCVD films from the metal alkyls were heavily oxidized due to the poor vacuum conditions employed in the early work. In order to concentrate on the characteristics unique to LCVD, only those systems which yielded films of good quality under a wide range of conditions such as the metal carbonyls and the H_2 reduction of WF_6 will be discussed in detail.

The cw CO_2 LCVD apparatus is shown in Fig. 2. Similar optical arrangements are used for LCVD with the pulsed CO_2 and cw Kr lasers. The laser is an electrically pulsed, line tunable cw CO_2 with maximum output power of 40 W. Attenuation of the beam is provided by current control and a wire grid polarizer. A removable power meter and or fluorescent viewing plates are used to check power stability and beam quality. A He-Ne beam is folded into the optical path with a ZnSe Brewster angle beam splitter to allow optical monitoring of the thickness of the LCVD film. Both beams are focused through a NaCl window onto the substrate with a 10 in. focal length 10.6 μm Ar-coated ZnSe lens. The CO_2 beam profile at the substrate was measured by pinhole scans and is approximately gaussian with a $D_{1/e^2} = 600$ μm. The beam diameter of the He-Ne laser at the focus is much smaller. The temporal intensity profile of the CO_2 pulses of several ms or longer was essentially a step function with some initial overshoot as measured using a HgCdTe detector. Because the amount of reactant used during LCVD is a small fraction of the total concentration, the depositions were carried out with closed reaction cells. Fused quartz is an excellent substrate material for LCVD using a CO_2 laser as it has a high absorption coefficient at 10.6 μm and is transparent in the visible for ease of optical monitoring, both visually and with the He-Ne laser. In addition, quartz has a low thermal conductivity which tends to further localize the deposition and a high resistance to thermal stress.

LCVD Ni

In earlier work in the LCVD of Ni from Ni $(CO)_4$ on quartz substrates using the cw CO_2 laser [1], it was found that the initial deposition rate was a constant with irradiation time for a constant intensity laser pulse as is shown in Fig. 3. This behavior is not what would be expected for deposition using an optical heat

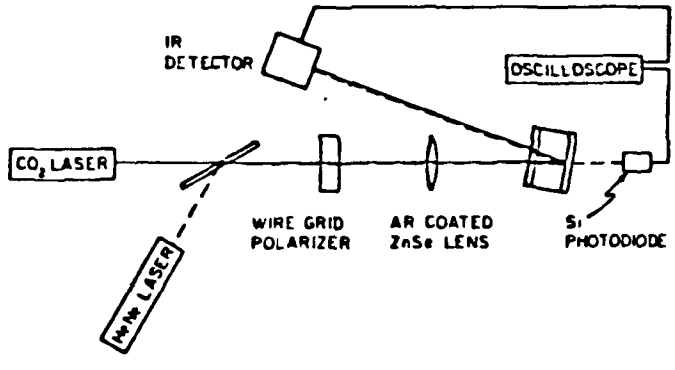

Fig. 2. Schematic diagram of the LCVD apparatus.

source. For the case of a reflecting (i.e., metal) film deposited on a highly absorbing substrate, the absorbed laser intensity and therefore the substrate temperature decreases as the film is deposited as shown in Fig. 4. As a result, the deposition rate should also decrease. The expected "optical self-limiting" of the film thickness has been observed in other systems, however, and will be discussed below.

Several other important points characteristic of LCVD are illustrated in Fig. 3. The initial deposition profile thickness is a truncated gaussian shape and reflects the temperature profile generated by the gaussian laser beam on the substrate. The diameter of the deposit can be much less than the corresponding beam diameter, however, because the deposition rate is a highly nonlinear, usually exponential, function of the substrate temperature. The result is a deposit thickness profile which has the shape of the central portion of a gaussian curve. This "resolution enhancement" effect is also observed in other laser deposition methods to some degree. LCVD spot diameters as small as 1/10 of the laser beam diameter have been observed.

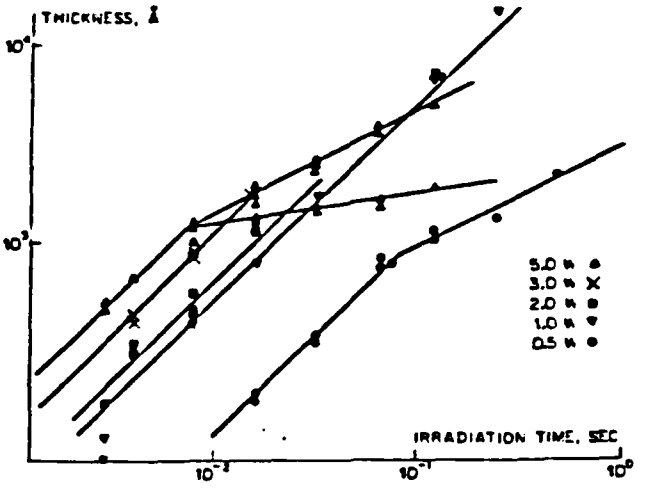

Fig. 3. Thickness of LCVD Ni films as a function of irradiation time. For the 5.0 W data, the upper curve is the maximum thickness and the lower curve is the thickness at the center of the spot. Similar branching is observed in the 3.0 and 2.0 W data but is not shown for reasons of clarity.

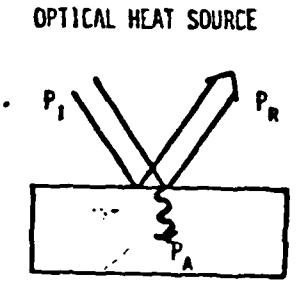

1. REFLECTOR/ABSORBER ---------- P_R INCREASES
   P_A DECREASES
2. ABSORBER/REFLECTOR ---------- P_R DECREASES
   P_A INCREASES
3. REFLECTOR/REFLECTOR
4. ABSORBER/ABSORBER ---------- P_R, P_A CONSTANT

Fig. 4. Absorptivity changes during LCVD for different film/substrate combinations.

At some point the curves of Fig. 3 change slope and split into two curves. The thickness profile for these "long" irradiation times changes smoothly from the truncated gaussian to a double humped "volcano" shape. The two curves therefore represent the maximum thickness and the center thickness of the volcano thickness profile. As the laser intensities used are not sufficient to melt either quartz or Ni and no evidence of melting is observed, the change in profile is ascribed to a depletion of reactants and build up of products at the center for the irradiated area and entrainment of reactants from the edges.

LCVD Fe

The thickness of LCVD Fe from $Fe(CO)_5$ [2] as a function of irradiation time, τ, for several laser powers is given in Fig. 5a. For irradiation times longer than the maximum given for each case, the deposition thickness profiles deviated significantly from the truncated gaussian shape observed for short irradiation times. In contrast to the similar data for Ni in Fig. 3, the thickness is not a linear function of the irradiation time and the lower intensity data (2.2 W) exhibits a steeper slope (thickness proportional to $\tau^{0.8}$) than the higher intensity points (5.5 W, thickness pro-

Table 1. Experimental Conditions for Laser Deposition

	LCVD	LEEP	LPD
Laser source	IR, VIS, near UV	VIS	UV, Multiphoton IR
Intensity (W/cm^2)	$10^2 - 10^6$	$10^4 - 10^5$	$10^{-3} - 10$
Reactant concentration (Torr)	10 - 760	—	0.1 - 10
Deposition rate (μm/sec)	0.1 - 100	≤10	≤0.01
Deposited	Ni[1], W[1,2] Cr[3], Mo[3], Al[3,4,5], Zn[4] Cd[4], Sn[3], Fe[2], Si[6], C[7], TiO_2[1] TiC[8], GaAs[8]	Ni[9], Cu[9] Au[9]	Cd[10], Zn[10]; Sn[10], Bi[10]; Al[10], W[10], Cr[10,1], Mo[1], Ga[10,13], As[13], GaAs[13] Si[10,14,15], Ge[10,15], SiO_2[12]

Table 2.

$$Sn(CH_3)_4 \longrightarrow Sn + CH_4$$

$$TiCl_4 + H_2 + CO_2 \longrightarrow TiO_2 + HCl + CO$$

$$TiCl_4 + CH_4 \xrightarrow{(H_2)} TiC + HCl$$

$$TiCl_4 + C_2H_2 + H_2 \longrightarrow TiC + HCl$$

$$Ga(CH_3)_3 + As(CH_3)_3 \xrightarrow{(H_2)} GaAs + CH_4$$

$$Ni(CO)_4 \longrightarrow Ni + CO$$

$$WF_6 + H_2 \longrightarrow W + HF$$

$$W(CO)_6 \longrightarrow W + CO$$

$$Fe(CO)_5 \longrightarrow Fe + CO$$

$$Al(CH_3)_3 \xrightarrow{(H_2)} Al + CH_4$$

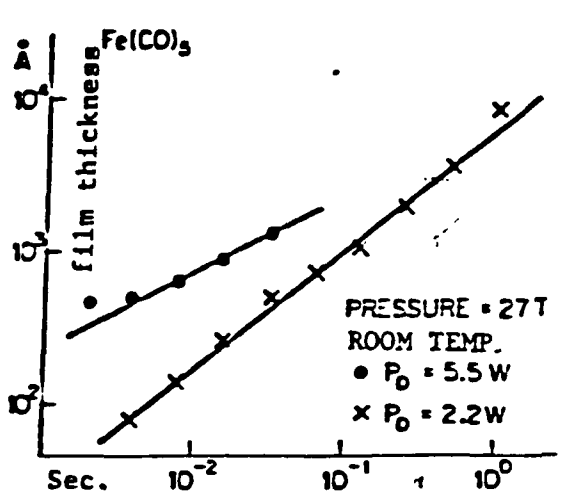

Fig. 5a. LCVD film thickness as a function of irradiation time (Fe from $Fe(CO)_5$).

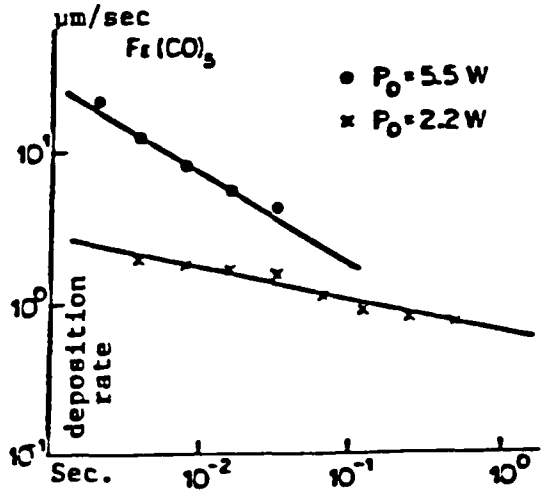

Fig. 5b. Apparent deposition rate (film thickness irradiation time) as a function of irradiation time (Fe from $Fe(CO)_5$).

portional to $\tau^{0,5}$). The same data is replotted in Fig. 5b as the apparent deposition rate, defined as the deposit thickness divided by the irradiation time. The actual deposition rate is a more complicated function of the heating time and the changing absorptivity of the surface during deposition, but this definition serves to illustrate qualitatively the optical self-limiting of the film thickness. For the shortest irradiation times, 2 ms, the higher incident laser intensity yields a faster deposition rate, in accord with the higher laser generated surface temperature. As the irradiation time increases, however, the deposited film reflects increasing amounts of the incident energy and the surface temperature decreases. The deposition rate should therefore approach a constant for long irradiation times. Before this point, however, other limiting mechanisms come into play. For example, as discussed above, diffusion processes may lead to a decreased reactant concentration at the center of the laser heated spot for relatively long irradiation times, resulting in decreased deposition at the spot center.

Another indication that optical self-limiting is occurring is given by experiments in which multiple irradiations of 3 ms each at 5.5 W incident power were made on a single site. After the initial deposition of approximately 500 Å, no additional deposition is observed. For the multiple depositions, the site is allowed to cool to ambient between each irradiation and the change in reflectivity from the uncoated quartz (R = 0.10) to several hundred Å

of Fe (R = 0.94) [19] would decrease the laser generated surface temperature by almost an order of magnitude. For the continuously irradiated site, the decrease in surface absorptivity occurs on an already heated substrate and the surface temperature decreases but may remain above the deposition temperature.

The LCVD Ni and Fe films were adherent, hard shiny, and metallic looking. Surface microstructure as determined by scanning electron microscopy (SEM) was essentially featureless to less than the resolution of the instrument (100 Å). The electrical resistivity of a 550 Å thick LCVD Ni film was measured as less than 4×10^{-5} ohm-cm but similar films of LCVD Fe showed high resistivities presumably due to oxidation of the relatively thin film.

LCVD W

LCVD of W from $WF_6 + H_2$ was carried out as a function of irradiation conditions for WF_6 pressures ranging from 40 to 200 T with a constant H_2 pressure of 400 T. The apparent deposition rate is plotted in Fig. 6 as a function of the irradiation time. In this case the deposition was carried out with the same laser intensity but with different concentrations of WF_6. The higher concentrations of WF_6 yielded greater initial deposition rates, as expected from kinetic considerations, which decreased faster with increasing irradiation time. For irradiation times on the order of 1 sec, the apparent deposition rate is the same for both reactant concentrations. (The lower pressure data for times greater than 1 sec is spuriously high because of buckling of the W films). This functional behavior is consistent with the optical self-limiting mechanism.

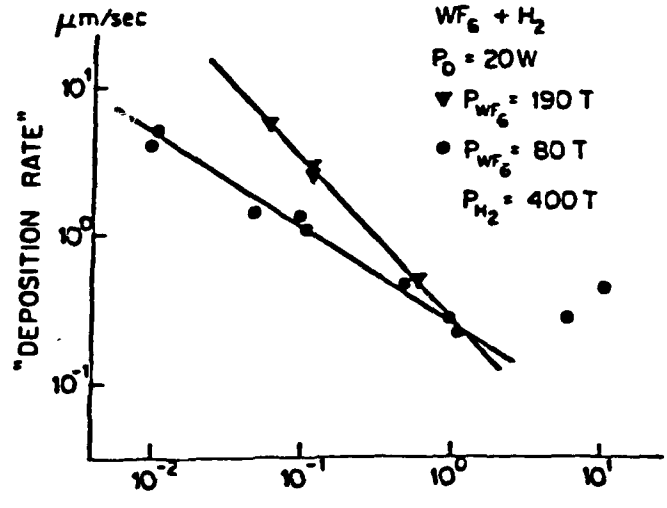

Fig. 6. Apparent deposition rate (film thickness/irradiation time) as a function of irradiation time (W from $WF_6 + H_2$).

Lines were generated by translating the substrate under the laser beam at speeds of 1 - 10 cm sec. Cross sectional profiles were approximately trapedzoidal with widths varying from 150 to 400 μm depending on scan speed and incident intensity. Resistivity measurements of lines 0.5 cm long, 600 Å thick, 400 μm wide and 1500 Å thick, 160 μm wide yielded 2×10^{-5} and 6×10^{-5} ohm-cm respectively. These numbers compare favorable to the bulk resistivity of W, $\rho = 6 \times 10^{-5}$ ohm-cm [19], particularly since the LCVD conditions have not been optimized. With the exception of irradiation times much greater than 1 sec, the LCVD films were quite adherent. Scanning electron microscope examination of the LCVD films revealed surface structure that varied from smooth (no observable features greater than 100 Å), to grandular nodules approximately 2000 Å in diameter (Fig. 7a) to small crystallites approximately 4000 Å (Fig. 7b) in diameter. This change in surface structure appears to be related to both irradiation conditions and diffusion processes with larger crystallites observed for longer irradiation times, as would be expected. The optical self-limiting of the $WF_6 + H_2$ LCVD reaction is graphically illustrated in Fig. 7. The film shown in Fig. 7b is only about 40% thicker than that of Fig. 7a although the reactant concentration is higher and the irradiation time is almost two orders of magnitude longer.

Experiments similar to those described above for LCVD W from $WF_6 + H_2$ have recently begun using Si substrates and a Kr ion laser. The blue-green lines (468 - 530 nm) of the Kr laser are strongly absorbed by the Si and most gaseous reactants are transparent in the visible, satisfying the LCVD requirements. The laser is focused with a 6.5 cm focal length lens onto the substrate with a beam diameter of approximately 20 μm at the focus. Lines and spots were deposited at scan speeds of 0.2 - 2.0 mm/sec at laser powers of 3 - 4 W. A curious growth pattern was observed for some spot depositions. Single crystal W spikes could be deposited with dimensions on the order of 40 - 50 μm wide and 50 - 120 μm tall. These are similar in aspect ratio to the polycrystalline C and Si rods deposited by LCVD by Bauerle et. al. [6,7], but the appearance of one or at most a few large crystals has not previously been observed. The growth rates measured for these crystallites approach a mm sec. The reason such structures have not been seen in the LCVD of W using the CO_2 laser is presumably due to the large difference in spot sizes - 600 μm for CO_2 and 20 μm for the Kr laser. If the incident laser beam impinges on only a few growing crystallites, it is reasonable that one or more would begin to dominate in the growth. Additional experiments are planned to quantify the irradiation conditions which favor such single crystal deposition.

10

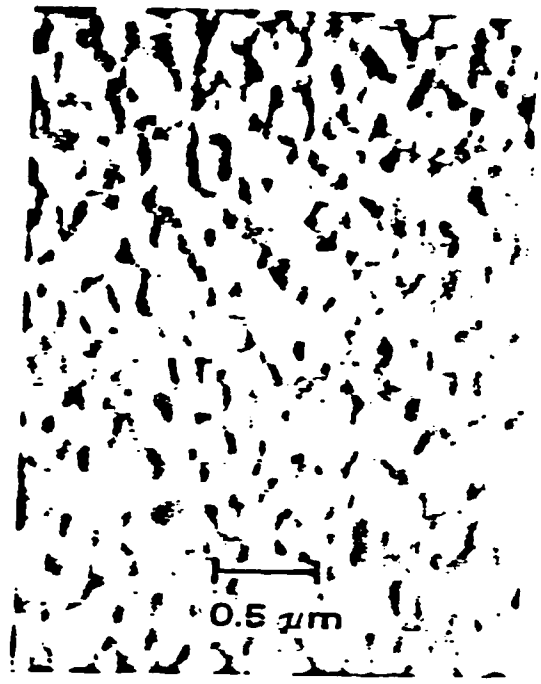

Fig. 7a. SEM photograph of LCVD W film (W from $WF_6 + H_2$, P = 20 W for 50 ms, 5 irradiations).

Fig. 7b. SEM photograph of LCVD W film (W from $WF_6 + H_2$, P = 20 W for 2 secs.)

LCVD GaAs

GaAs was deposited using the reactions: $Ga(CH_3)_3 + As(CH_3)_3 + H_2 \rightarrow GaAs + CH_4$. Both $Ga(CH_3)_3$ and $As(CH_3)_3$ were distilled into the side-arm of the deposition cell and 150 T of H added. The side arm of the cell was maintained at 0°C and the vapor pressures of $Ga(CH_3)_3$ and $As(CH_3)_3$ were 65 and 98 T, respectively. The range of irradiation conditions over which deposition was observed was quite narrow: $D_1/e^2 \simeq 0.6$ mm; P_0 = 2-3 W; and τ = 2-12 s. For higher incident powers, deposition occurred in a ring around a center devoid of measurable GaAs. The surface temperatures achieved under these irradiation conditions are approximately the same as used for conventional MO CVD [20] 600-900°C.

The LCVD films were not continuous and showed a strong effect of nucleation sites on the substrate. The scratches on the surface of the substrate are readily apparent in the growth of the film. This type of deposition has been observed in conventional CVD on similar substrates [2]. Deposition rates were much slower than observed for other LCVD materials: [1] 150-500 Å/s, but were comparable to rates observed in conventional MOCVD [20]. Film thickness could be built up by multiple irradiations of the same site,

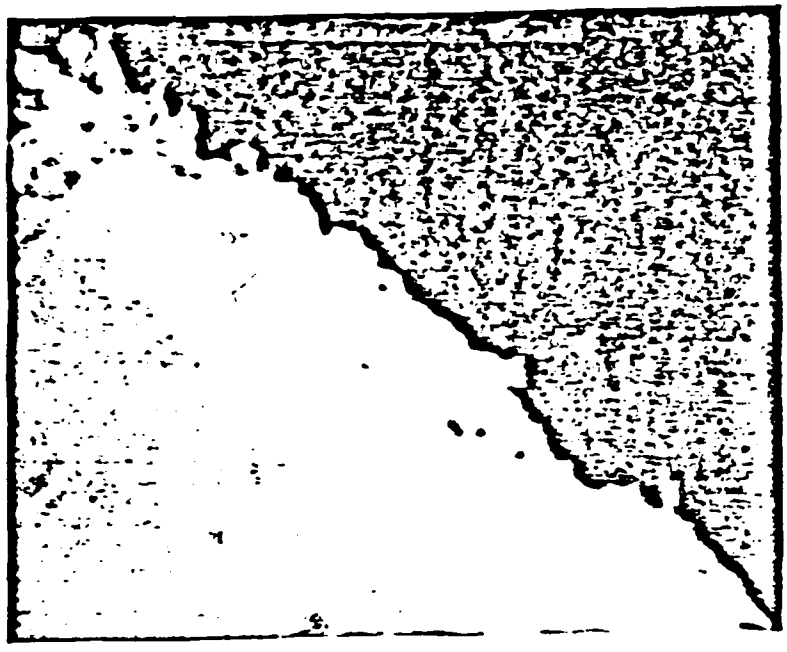

Fig. 8a. SEM photograph of fracture cross section of LCVD TiC film on carbon steel ($TiCl_4 + CH_4$).

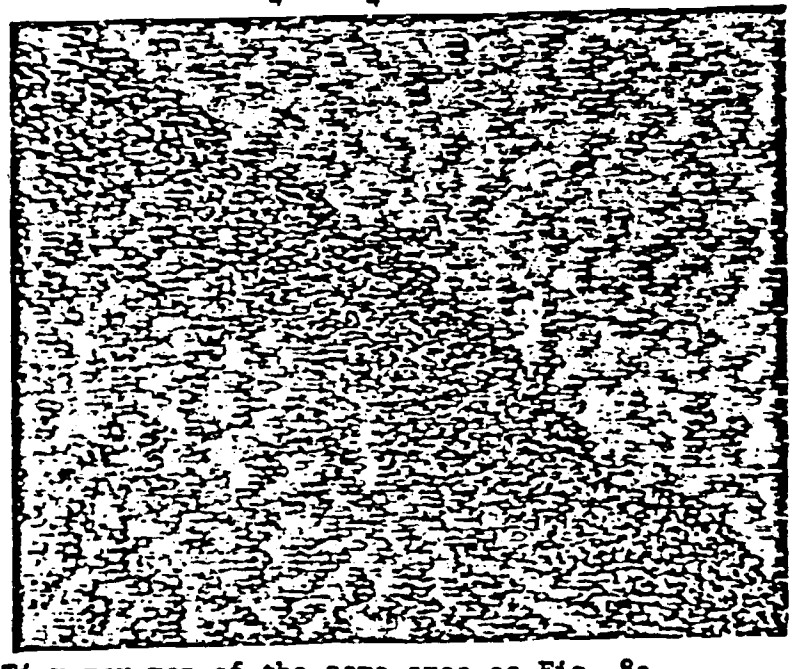

Fig. 8b. Ti x-ray map of the same area as Fig. 8a

site, resulting in films several microns thick and better but not complete coverage. In one case, the laser irradiated a site where some of the liquid material had condensed. The deposition rate observed was several orders of magnitude greater than in a "clean" site. The composition of the LCVD GaAs films was analyzed using SEM/EDAX. The Ga/As ratio varied with irradiation conditions from 0.3 to 2.0, bracketing the value of pure GaAs, 0.73.

LCVD TiC and TiO_2

In order to deposit TiC on carbon steel substrates, several orders of magnitude more laser power is necessary due to the decreased absorptivity and increased thermal diffusivity of the steel relative to quartz. TiC was deposited from TiCl at the room temperature vapor pressure of 12 T and CH_4 or C_2H_2 (200 T) with and without H_2 (200 T). The high power LCVD apparatus consisted of a stainless steel tank electroless Ni plated with x and y translation stages driven by an external stepping motor. Coating tracks were deposited by translating the substrate under the stationary CO_2 laser beam. Incident powers were 500-1200 W, D_1/e^2 = 1-2 mm and translation speeds of 3-6 mm/s.

A SEM of the fracture cross section of a typical LCVD TiC track is given in Fig. 8(a) along with the Ti x-ray map of the same area (Fig. 8(b)). The Ti is concentrated in the fine grained region shown in Fig. 8(a) which corresponds to the LCVD TiC coating. The fine grained material has a grain size of 500-1000 Å. These LCVD tracks show increased surface hardness but are not thick enough (typically 0.5-1.0μ) for the hardness to be measured directly.

TiO_2 was deposited from $TiCl_4 + CO_2 + H_2$. TiCl was vacuum distilled into a side-arm tube of the deposition cell and 205 T each of CO_2 and H_2 added. The partial pressure of $TiCl_4$ was 12.4 T, the room temperature vapor pressure. The irradiation conditions were: laser beam diameter D_1/e^2 = 0.8-3.0 mm; laser power P = 5-10 W; and irradiation time τ = 0.1-1.0 s. The measured deposition rate was 300-3000 Å/s. The LCVD TiO_2 films were clear and adherent. Other properties are given in Ref. 1.

Optical Monitoring of LCVD

Using the apparatus shown in Fig. 2, the LCVD film growth was monitored in real time by monitoring both the reflected CO_2 beam using a Ge:Au or HgCdTe detector and the transmitted He-Ne beam using a Si photodiode.

Representative transmission and reflection curves are given in Fig. 9 for the W from $WF_6 + H_2$ system for different laser intensities and an irradiation time of nominally 100 ms. The upper curve is the He-Ne intensity and the lower curve the reflected CO_2 intensity as measured by a Ge:Au detector. At the lower incident power (Fig. 9a) a delay time of approximately 67 msec is observed before significant deposition takes place as evidenced by a steep decrease in the He-Ne transmission and an increase in the CO_2 reflectance. (The initial decay in the transmission is due to substrate heating and subsequent defocusing of the He-Ne beam.) A comparison of the delay times for several different incident intensities showed that the data could be fit by a very simple model assuming no deposition until a "threshold temperature" was reached and one dimensional heat flow in the laser heated substrate. Under these conditions, the surface temperature is proportional to the incident intensity and the square root of the irradiation time if we further assume that the optical and thermal properties of the quartz substrate are constant. As shown in Table 3, the product of the incident power and the square root of the delay time before deposition takes place is a constant, indicating that there is some validity to the simple model. Similar calculations of the actual surface temperature for a gaussian beam do not yield reasonable numbers however [22]. For quartz it is necessary to take into account the temperature dependence of the thermal properties

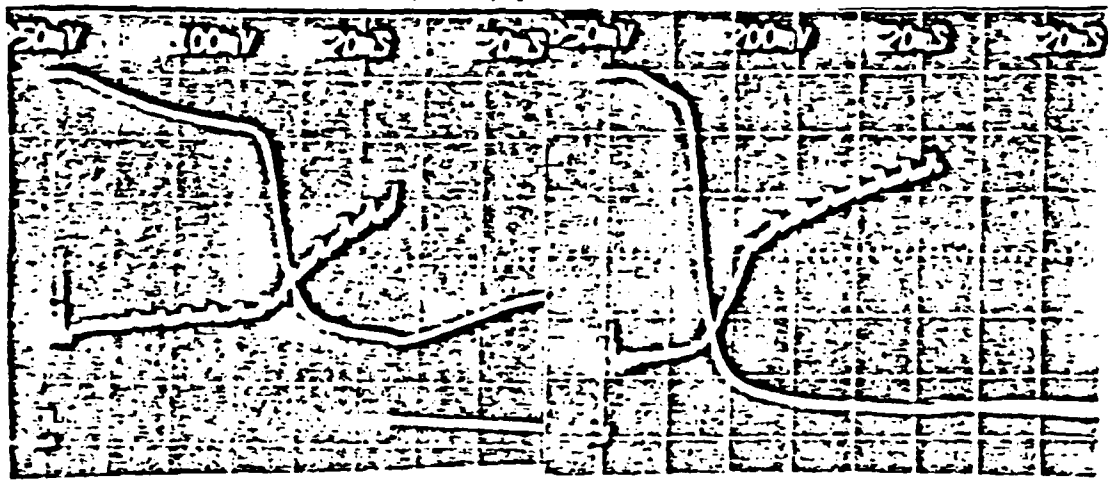

(a) (b)

Fig. 9. Transmission and reflection vs. time curves for cw LCVD of W from $WF_6 + H_2$ (rt T, 400 T). The upper curve is the He-Ne transmission intensity and the lower curve the CO_2 reflected intensity. Laser power: a) 4.7 W; b) 7.0 W.

such as heat capacity and thermal diffusivity. Such nonlinear calculations yield surface temperatures for the experimental conditions of Table 3 of 800 - 950°C [23], in good agreement with temperatures used in conventional CVD [24].

Table 3. Relative surface temperature, T_s, for different irradiation conditions (W from $WF_6 + H_2$).

RELATIVE T_s FOR $WF_6 + H_2$ LCVD

P (watts	τ (msec)	$P\tau^{\frac{1}{2}} \propto T_s$
4.7	55.8	35.1
7.0	22.5	33.2
10.0	10.9	33.0
15.0	4.9	33.2

A representative transmission and reflection curve for LCVD Fe from $Fe(CO)_5$ is given in Fig. 10. In this case there is a similar delay time before depositon begins (approximately 35 msec) but the deposition is much slower and continues for several hundred milliseconds. The calculated surface temperature before deposition begins for the irradiation conditions of Fig. 10 is 500°C. For the lower laser power used in the Fe from $Fe(CO)_5$ LCVD experiment there is no observable thermal defocusing of the He-Ne beam.

CONCLUSIONS

From a comparison of both the thickness vs. irradiation time data and the real time optical monitoring of the deposition initiation and rate for the several deposition systems examined, some general conclusions can be drawn. For the low temperature reactions such as the Ni from $Ni(CO)_4$ deposition, the laser generated substrate temperature after the deposition of a reflecting metal film is still above the threshold temperature for the reaction. The initial LCVD rate in this case must be very rapid and the optical self-limiting must occur for irradiation times shorter than the 3 msec used [1]. The linear dependence of deposition rate with irradiation time can be attributed to the substrate temperature reaching an effective equilibrium. For the higher temperature reactions such as W from $WF_6 + H_2$, there is a delay (Table 2) before the substrate temperature reaches the threshold temperature

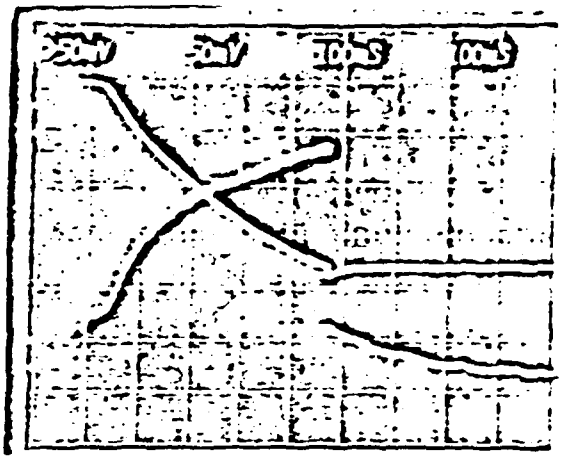

Fig. 10. Transmission and reflection vs. time curves for cw LCVD of Fe from $Fe(CO)_5$ (27 T). The upper curve is the He-Ne transmission intensity and the lower curve the CO_2 reflected intensity. Laser power is 2 W.

of the reaction. The change in optical absorption with LCVD film growth of several hundred Å lowers the substrate temperature below the threshold temperature, and film growth ceases. The Fe from $Fe(CO)_5$ case lies between these two extremes. This simple picture ignores any kinetic or chemistry effects which may be observed. The model does, however, give a general picture of the optical and thermal properties which must be taken into account in LCVD.

Applications for LCVD films will depend not only on the localization property of the technique but also on the ability to generate different film microstructures using the rapid heating and cooling rates available with a laser heat source. It is possible to deposit films with dimensions less than the diameter of the depositing laser focal spot due to the exponential dependence of the deposition rate on temperature. For properly chosen irradiation conditions, the LCVD film will only be deposited in the center of the laser heated hot spot on the substrate surface [1]. Spot sizes of 1/10 of the beam have been observed. In order to utilize this resolution enhancement, short irradiation times are necessary, where short is defined in terms of the thermal diffusivity of the substrate. LCVD experiments with a pulsed CO_2 TEA laser have shown that irradiation times as short as 1 μsec can be used to deposit useful film thicknesses for some reaction systems, thereby minimizing lateral thermal spreading.

The rapid deposition rates measured for LCVD are a consequence of several factors. High surface temperatures can be achieved because only a small area is heated, effectively suppressing gas phase reactions in favor of surface reactions. For the same reasons, high concentrations of reactants can be utilized. A

third effect is the enhanced diffusion of reactants inherent in the spot geometry of the reaction site as opposed to the planar geometry of conventional CVD. The increase in diffusion of reactants should be a function of the irradiated spot size with smaller deposit geometries exhibiting faster deposition rates.

Initial results on the LCVD of compounds have not been as promising as those obtained for metal films, with deposition rates being an order of magnitude or more smaller. Additional experiments are planned for these more complex systems.

Possible applications for LCVD coating include: IC mask and circuit repair; writing interconnects for IC circuits; one-step ohmic contacts; localized protective coatings; localized coatings for waveguide optics; and localized wear and corrosion resistant coatings.

Acknowledgements

This work was supported in part by a grant from AFOSR under the technical cognizance of H. Schlossberg.

REFERENCES

1. S. D. Allen, J. Appl. Phys. 52, 6501 (1981) and references therein.
2. S. D. Allen and A. B. Trigubo, J. Appl. Phys. (Feb. 1983)
3. S. D. Allen and A. B. Trigubo, unpublished results.
4. Y. Rytz-Froidevaux, R. P. Salathé, and H. H. Gilgen, Phys. Lett. 84A, 216 (1981).
5. R. W. Bigelow, J. G. Black, C. B. Duke, W. R. Salaneck and H. R. Thomas, Thin Sol. Films 94, 233 (1982).
6. C. P. Christensen and K. M. Lakin, Appl. Phys. Lett. 32, 254 (1978); V. Baranauskas, C.I.Z. Mammana, R. E. Klinger, and J. E. Greene, Appl. Phys. Lett. 36, 920 (1980); D. J. Ehrlich, R. M. Osgood, Jr., and T. F. Deutsch, Appl. Phys. Lett. 39, 957 (1981); D. Bauerle, P. Irsigler, G. Leyendecker, H. Noll, and D. Wagner, Appl. Phys. Lett. 40, 819 (1982).
7. G. Leyendecker, D. Bauerle, P. Geittner and H. Lydtin, Appl. Phys. Lett. 39, 921 (1981).
8. S. D. Allen and A. B. Trigubo, J. Vac. Sci. Tech. 20, 469 (1982).
9. R. J. von Gutfeld, R. E. Acosta, and L. T. Romankiw, IBM J. of Res. and Dev. 26, 136 (1982); J. C. Puippe, R. E. Acosta and R. J. von Gutfeld, J. Electrochem. Soc. 128, 2539 (1981); R. J. von Gutfeld, E. E. Tynan, R. L. Melcher, and S. E. Blum, Appl. Phys. Lett. 35, 651 (1979).

10. T. F. Deutsch, D. J. Ehrlich, and R. M. Osgood, Jr., Appl. Phys. Lett. 35, 175 (1979); D. J. Ehrlich, R. M. Osgood, Jr., and T. F. Deutsch, J. Vac. Sci. Tech. 21, 23 (1982); D. J. Ehrlich, R. M. Osgood, Jr., and T. F. Deutsch, IEEE J. Quant. Elec. QE-16, 1233 (1980) and references therein.
11. R. Solanki, P. K. Boyer, J. E. Mahan and G. J. Collins, Appl. Phys. Lett. 38, 572 (1981); R. Solanki, P. K. Boyer, and G. J. Collins, Appl. Phys. Lett. 41, 1048 (1982).
12. P. K. Boyer, G. A. Roche, W. H. Ritchie and G. J. Collins, Appl. Phys. Lett. 40, 716 (1982); P.K. Boyer, W. H. Ritchie, and G. J. Collins, J. Electrochem. Soc. 129, 2155 (1982).
13. J. G. Berg, P. Yeung, and S. D. Allen, TRW, El Segundo, CA, unpublished results.
14. M. Hanabusa, A. Namiki, and Keitaro Yoshihara, Appl. Phys. Lett. 35, 626 (1979).
15. R. W. Andreatta, C. C. Abele, J. F. Osmundsen, J. G. Eden, D. Lubben and J. E. Greene, Appl. Phys. Lett. 40, 183 (1982).
16. See also Proceedings of the MRS Symposium on Laser Diagnostics and Photochemical Processing for Semiconductor Devices (11-82), North Holland, New York.
17. R. H. Micheels, A. D. Darrow, and R. D. Rauh, Appl. Phys. Lett. 39, 418 (1981).
18. R. F. Karlicek, V. M. Donnelly, and G. J. Collins, J. Appl. Phys. 53, 1084 (1982).
19. American Institute of Physics Handbook, ed. by D. E. Gray (McGraw-Hill, New York, 1972).
20. P. D. Dapkus, H. M. Manasevit, and K. L. Hess, J. Cryst. Growth 55, 10 (1981).
21. P. D. Dapkus, private communication.
22. J. F. Ready, Effects of High-Power Laser Radiation (Academic Press, New York, 1971).
23. S. D. Allen and J. Goldstone, to be published.
24. C. F. Powell, J. H. Oxley and J. M. Blocher, Jr., Vapor Deposition (Wiley, New York, 1968).

LASER CHEMICAL VAPOR DEPOSITION USING CW AND PULSED LASERS

S. D. Allen, A. B. Trigubo, and Y.-C. Liu
Center for Laser Studies, University of Southern California
University Park, DRB 17, Los Angeles, CA 90089-1112

Abstract

The deposition rate in laser chemical vapor deposition (LCVD) is a function of the surface temperature and therefore also a function of the changing reflectivity of the surface during deposition. The influence of these parameters on the LCVD rate of metallic and insulating thin films was investigated using both pulsed and cw laser sources and optical monitoring of the depositing film thickness. Physical properties of the LCVD films are reported.

LASER CHEMICAL VAPOR DEPOSITION USING CW AND PULSED LASERS

Susan D. Allen

Center for Laser Studies, University of Southern California,

University Park, DRB 17, Los Angeles, CA 90089-1112

Introduction

Laser chemical vapor deposition (LCVD) is one of several recently developed techniques for direct writing of thin film structures with small radial dimensions utilizing a laser to effect a localized deposition [1,2,3,4]. Laser deposition can be conveniently divided into two types: thermal and photochemical. A generalized laser deposition experimental arrangement is given in Fig. 1. For thermally driven laser deposition such as LCVD [1] and laser enhanced electroplating [2] the laser wavelength is chosen such that the reactants are transparent and the substrate absorbing. Focusing the laser on the substrate creates a localized hot spot at which the deposition takes place. For laser photochemical deposition (LPD) the reverse conditions apply - the laser energy is absorbed by the reactants and the substrate is transparent. The focused laser creates a high concentration of reactive species near the substrate, causing localized deposition. The advantages of laser deposition are, in general, those associated with other laser processing techniques: a) spatial resolution and control; b) availability of rapid, i.e., nonequilibrium, deposition conditions; c) localization of heating in the thermal processes or low temperature processing in LPD; d) increased purity of the

deposits; and e) ability to interface easily with other laser processing techniques such as laser annealing and contact formation in semiconductors and laser processing of metals and ceramics.

LCVD of metals, insulators and semiconductors has previously been reported [1,5]. For the LCVD of Ni from $Ni(CO)_4$ [1] on quartz substrates using a cw CO_2 laser, it was found that the deposition rate was a constant with irradiation time for a constant intensity. This behavior is not would be expected for deposition using an optical heat source. For the case of a reflecting, i.e., metal film, deposited on a highly absorbing substrate, the absorbed laser intensity and therefore the substrate temperature decreases as the film is deposited and the deposition rate should also decrease. We report here the LCVD of Fe and W films and the observation of optical self-limiting of the film thickness for some irradiation conditions.

LCVD depositions were carried using both the apparatus previously described [1] and a modification described below. The new apparatus utilizes an electrically pulsed, tunable cw CO_2 laser with maximum output power of 40 W. Attenuation of the beam was provided by a wire grid polarizer. A removable power meter and/or fluorescent viewing plates were used to check power stability and beam quality. The beam was focused onto the absorbing substrate with a 10 in. focal length AR-Coated ZnSe lens through a NaCl window. The beam profile at the substrate was approximately Gaussian with a

D_{1/e^2} = 600 μm. For pulses of 1 ms or longer the temporal intensity profile was approximately a step function with a small amount of overshoot as measured using a HgCdTe detector. The reactions studied include those shown in Table 1. The temperatures given for the reactions are the minimum recommended deposition temperatures for the conventional CVD process [6]. Because the amount of reactant used during LCVD is a small fraction of the total concentration, the depositions were carried out with closed reaction cells.

LCVD Fe

$Fe(CO)_5$, a liquid at room temperature, was vacuum distilled into a side arm of the deposition cell using a vacuum system with a base pressure of 5×10^{-6} T. Care was taken to avoid illumination of the cell with fluorescent light in order to suppress the photochemical formation of $Fe_2(CO)_5$ [7,8]. Room temperature vapor pressure of 27 T was used for all deposition measurements [9].

The thickness of the LCVD Fe films as a function of irradiation time, τ, for two laser powers is given in Fig. 2a. For irradiation times longer than the maximum in each case, the deposition thickness profiles deviated significantly from the truncated gaussian shape observed [1] for short irradiation times. In contrast to the similar data for Ni [1], the thickness is not a linear function of the irradiation time and the lower intensity data (2.2 W) exhibits a steeper slope (thickness α $\tau^{0.8}$) than the higher intensity points (5.5 W, thickness α $\tau^{0.5}$). The same data is replotted in Fig. 2b as the apparent deposition rate, defined as the deposit thickness divided

by the irradiation time. The actual deposition rate is a more complicated function of the heating time and the changing absorptivity of the surface during deposition, but this definition serves to illustrate qualitatively the optical self-limiting of the film thickness. For the shortest irradiation time, 2 ms, the higher incident laser intensity yields a faster deposition rate, in accord with the higher laser generated surface temperature. As the irradiation time increases, however, the deposited film reflects increasing amounts of the incident energy and the surface temperature eventually declines. The deposition rate should therefore approach a constant for long irradiation times. Before this point, however, other limiting mechanisms come into play. For example, diffusion processes may lead to a decreased reactant concentration at the center of the laser heated spot for relatively long irradiation times, resulting in decreased deposition at the spot center. This phenomenon has been observed as changes in the LCVD film thickness profile from truncated gaussian to flat topped to a volcano shape with increasing irradiation time for most systems observed [1].

Another indication that optical self-limiting is occurring is given by the data of Fig. 3. Multiple irradiations of 3 ms each at 5.5 W incident power were made on a single site. After the initial deposition of approximately 500 Å, no additional deposiiton is observed. For the multiple depositions, the site is allowed to cool to ambient between each irradiation and the change in reflectivity from the uncoated quartz

(R = 0.04) to several hundred Å of Fe (R = 0.94) [10] would decrease the laser generated surface temperature by an order of magnitude or more.

The deposited spots and lines were adherent, hard, shiny and metallic looking. Resistivity measurements on lines generated by translating the substrate under the laser beam, however, showed very high resistivities which increased with time, implying heavy oxidation of the thin (250 Å) lines.

LCVD W

LCVD of W from $WF_6 + H_2$ was carried out as a function of irradiation conditions for WF_6 pressures ranging from 40 to 200 T. The apparent deposition rate is plotted in Fig. 4 as a function of the irradiation time. In this case the deposition was carried out with the same laser intensity but with different concentrations of WF_6. The higher concentration of WF_6 yielded a greater initial deposition rate, as expected from kinetic considerations, which decreased faster with increasing irradiation time. For irradiation times on the order of 1 sec, the apparent deposition rate is the same for both reactant concentrations. (The lower pressure data for times greater than 1 sec is spuriously high because of buckling of the W films). This functional behavior is consistent with the optical self-limiting mechanism.

Lines were again generated by translating the substrate under the laser beam at speeds of 1 - 10 cm/sec. Cross sectional profiles were approximately trapezoidal with widths

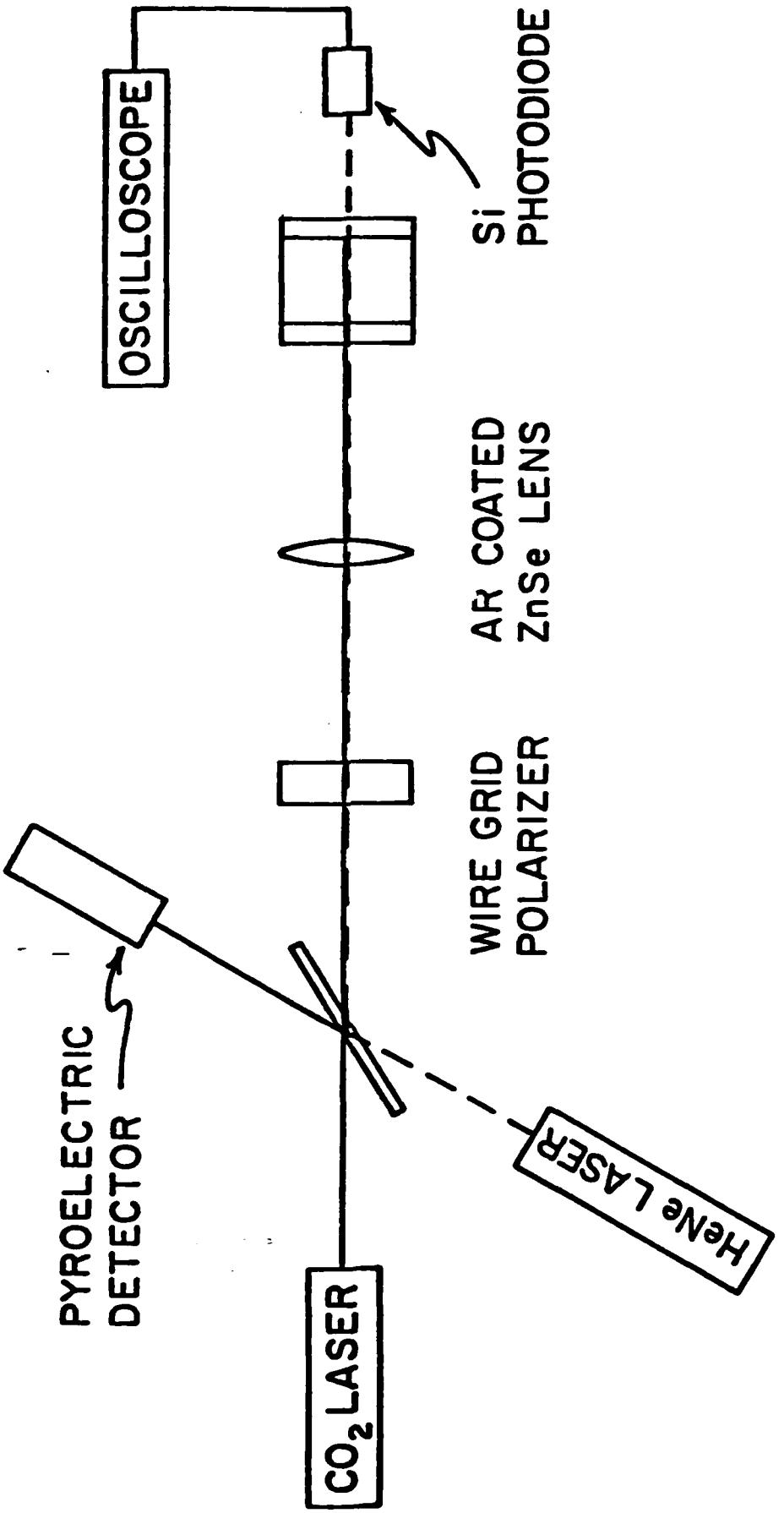
OSCILLOSCOPE
Si
PHOTODIODE
AR COATED
ZnSe LENS
WIRE GRID
POLARIZER
PYROELECTRIC
DETECTOR
HeNe LASER
CO_2 LASER

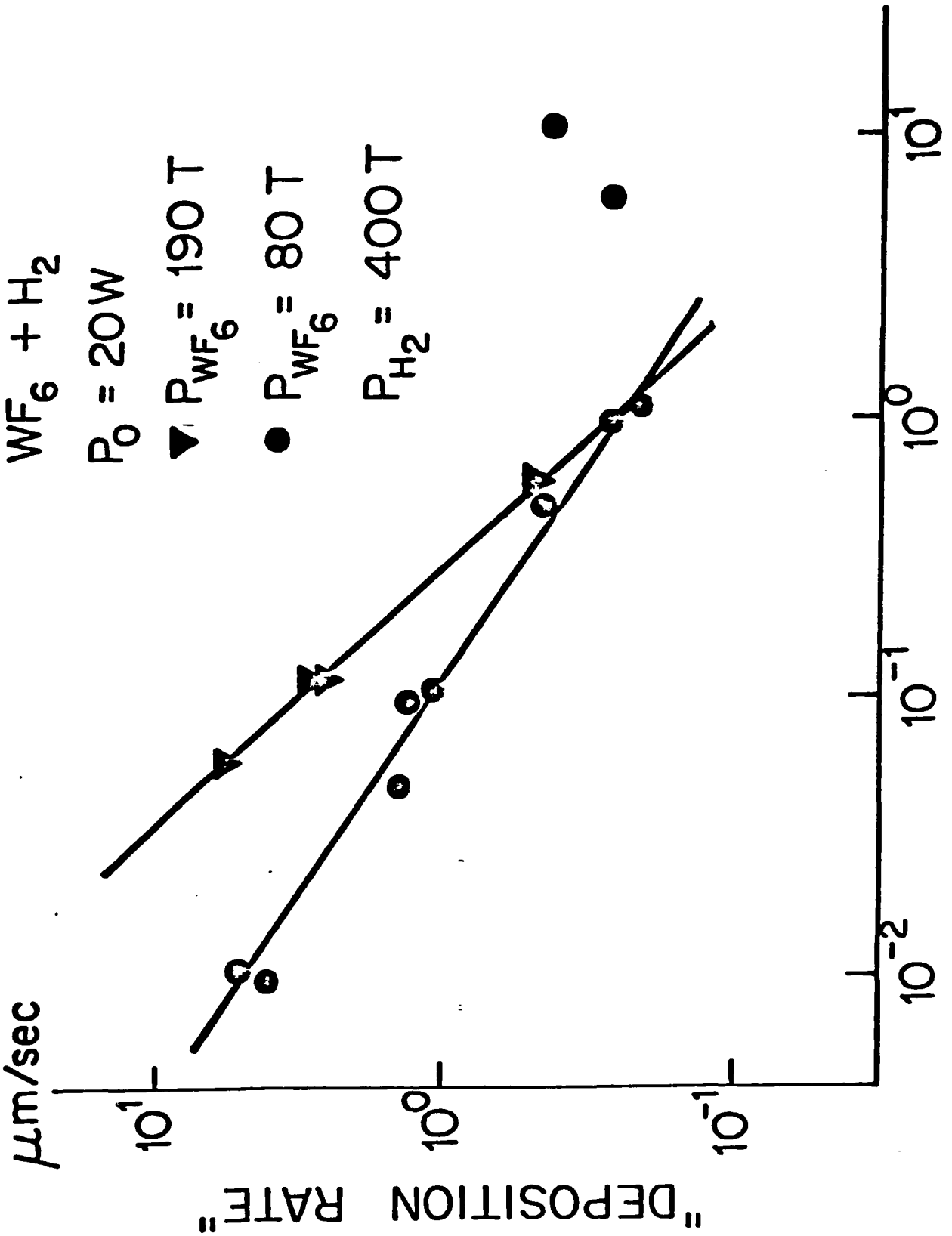
WF6 + H2
P0 = 20W
▶ PWF6 = 190 T
● PWF6 = 80 T
PH2 = 400T
"DEPOSITION RATE"
μm/sec
10-1
100
10-1
10-2
100
10-1

varying from 150 to 400 μm depending on scan speed and incident intensity. Resistivity measurements of lines 0.5 cm long, 600 Å thick, 400 μm wide; and 1500 Å thick, 160 μm wide yielded 2×10^{-5} and 6×10^{-5} ohm-cm respectively. These numbers compare favorably to the bulk resistivity of W, $\rho = 6 \times 10^{-6}$ ohm-cm [10], particularly since the LCVD conditions have not been optimized. With the exception of irradiation times much greater than 1 sec, the LCVD films were quite adherent. Scanning electron microscope (SEM) examination of the LCVD films revealed surface structure that varied from essentially featureless (to less than 100 Å) to grandular nodules approximately 1000 Å in diameter to small crystallites approximately 3000 Å in diameter. This change in surface structure appears to be related to both irradiation conditions and diffusion processes [11].

Only preliminary data has been obtained on LCVD W from $W(CO)_6$ because of several complications. A solid at room temperature, $W(CO)_6$ has a vapor pressure of less than 0.1 T at 30°C [8]. The deposition rate observed for such a low concentration was very low, requiring several seconds to deposit a visible metallic film. At the higher pressures obtained with a heated deposition cell (P = 20 T at 105°C), there is significant absorption of the 10.6 μm wavelength [13]. Experiments at other wavelengths are in progress.

PULSED LCVD

In order to unerstand the dynamics of the LCVD process a CO_2 TEA laser was used to heat the substrate. With a short

pulsed laser heat source, it is possible to heat the substrate to the deposition temperature before significant deposition takes place and then monitor the growth of the film after the laser pulse. Quartz substrates were chosen for the deposition because of their transparency in the visible, allowing optical monitoring of the film thickness, and because quartz has a very low thermal diffusivity. The short pulse laser heating will thus create a step function in the surface temperature which will decay with a time constant on the order of milliseconds.

The experimental apparatus for pulsed LCVD is shown in Fig. 5. The CO_2 TEA laser is operated as a stable resonator and generates 0.3 J. As measured by burn patterns and pinhole scans, the laser spatial distribution is approximately TEM_{00} and the total pulse length about 1 μsec. The He-Ne monitoring beam is folded into the CO_2 beam using a ZnSe Brewster angle beam splitter. The small percentage of the CO_2 beam reflected from the beam splitter as measured with a pyroelectric detector, serves as a monitor of shot to shot reproducibility. Attenuation of the intensity incident on the substrate is accomplished with a wire grid polarizer. The He-Ne transmission of the depositing film and therefore the optical thickness is measured with a Si photodiode and displayed on an oscilloscope. The AR coated, 10 inch focal length lens was positioned so that the He-Ne beam was focused on the substrate surface, yielding a relatively large CO_2 laser spot size (D_{1/e^2} = 650 μm).

The transmission of the He-Ne monitor beam vs. time for

several different CO_2 incident energies is shown in Fig. 6 for the system Ni from $Ni(CO)_4$ (pressure = 40 T) [1]. Instead of the expected single intensity decay curve, two separate decay curves are observed for the higher energy laser pulses and neither is simple. For low energies (Fig. 6e,d) there is an induction period before deposition begins. At higher energies, (Fig. a-c) an initial deposition takes place, but deposition stops and then continues after a delay time. The total LCVD film thickness scales with the incident energy with maximum thickness achieved before damage to the substrate of several hundred Å. Smilar results have been observed for deposition from 80 T of $Ni(CO)_4$. Pulsed LCVD using the system Fe from $Fe(CO)_5$ yielded transmission vs. time curves with only one decay region.

Although there is some contribution to the initial decay region observed for pulsed LCVD $Ni(CO)_4$ from defocusing of the He-Ne beam due to the creation of a thermal lens in the laser heated substrate, this effect alone does not explain the deposition behavior. Experiments are currently in progress to determine whether the observation of these two deposition regimes is a function of the chemistry of the $Ni(CO)_4$ pyrolysis reaction.

CW LCVD

Using an apparatus similar to that shown in Fig. 5 for the pulsed LCVD experiment, the film growth was monitored in real time using the cw laser previously described. In this case both the reflected CO_2 beam and the He-Ne monitoring

beam are measured during the laser pulse. Representative transmission and reflection curves are given in Fig. 7 for the W from $WF_6 + H_2$ system for different laser intensities and an irradiation time of nominally 100 ms. The upper curve is the He-Ne intensity and the lower curve the reflected CO_2 intensity as measured by a Ge:Au detector. At the lower incident power (Fig. 7a) a delay time of approximately 67 msec is observed before significant deposition takes place as evidenced by a steep decrease in the He-Ne transmission and an increase in the CO_2 reflectance. (The initial decay in the transmission is due to gas phase and substrate heating and subsequent defocusing of the He-Ne beam.) A comparison of the delay times for several different incident intensities showed that the data could be fit by a very simple model assuming no deposition until a "threshold temperature" was reached and one dimensional heat flow in the laser heated substrate. Under these conditions, the surface temperature is proportional to the incident intensity and the square root of the irradiation time if we further assume that the optical and thermal properties of the quartz substrate are constant. As shown in Table 2, the product of the incident power and the square root of the delay time before deposition takes place is a constant, indicating that there is some validity to the simple model. Similar calculations of the actual surface temperature for a gaussian beam do not yield reasonable numbers, however [13]. For quartz it is necessary to take into account the temperature dependence

of the thermal properties such as heat capacity and thermal diffusivity. Such non-linear calculations yield surface temperatures for the experimental conditions of Table 2 of 800-950°C [14], in good agreement with temperatures used in conventional CVD [6].

A representative transmission and reflection curve for LCVD Fe from $Fe(CO)_5$ is given in Fig. 8. In this case there is a similar delay time before deposition begins (approximately 35 msec) but the deposition is much slower and continues for several hundred milliseconds. The calculated surface temperature before deposition begins for the irradiation conditions of Fig.8 is 500°C [14]. For the lower pressure (approximately 27 T) and laser intensity used in the Fe from $Fe(CO)_5$ LCVD experiment there is no observable thermal defocusing of the He-Ne beam.

Conclusions

From a comparison of both the thickness vs. irradiation time data and the real time optical monitoring of the deposition initiation and rate for the several deposition systems examined, some general conclusions can be drawn. For the low temperature reactions such as the Ni from $Ni(CO)_4$ deposition, the laser generated substrate temperature after the deposition of a reflecting metal film is still above the threshold temperature for the reaction. The initial LCVD rate in this case must be very rapid and the optical self-limiting must occur for irradiation times shorter than the 3 msec used [1]. The linear dependence of deposition rate with irradiation time can be attributed to the substrate temperature reaching an effective equilibrium. For

the higher temperature reactions such as W from $WF_6 + H_2$, there is a delay (Table 2) before the substrate temperature reaches the threshold temperature of the reaction. The change in optical absorption with LCVD film growth of several hundred Å lowers the substrate temperature below the threshold temperature and film growth ceases. The Fe from $Fe(CO)_5$ case lies between these two extremes.

This simple picture ignores any kinetic or chemistry effects which may be observed. In particular, the two different deposition rates measured for the pulsed LCVD of Ni from $Ni(CO)_4$ are not explained. The model does, however, give a general picture of the optical and thermal properties which must be taken into account in LCVD.

Applications for LCVD films will depend not only on the localization property of the technique but also on the ability to generate different film microstructures using the rapid heating and cooling rates available with a laser heat source. It 's possible to deposit films with dimensions less than the diameter of the depositing laser focal spot due to the exponential dependence of the deposition rate on temperature. For properly chosen irradiation conditions, the LCVD film will only be deposited in the center of the laser heated hotspot on the substrate surface [1]. Spot sizes of 1/10 the size of the beam have been observed. In order to utilize this resolution enhancement, short irradiation times are necessary, where short is defined in terms of the thermal diffusivity of the substrate. The pulsed LCVD data show that irradiation times as short as 1 μsec can be used to deposit useful film thickness, minimizing lateral thermal spreading.

Initial results of LCVD of TiC on steel [5] indicate that fine-grained (1000 Å) films can be deposited with good adherence. However, the film deposited to date have been too thin to exhibit a significant hardening effect. Further experiments in localized deposition of hard coatings are planned.

Possible applications for LCVD coating include: IC mask and cricuit repair; writing in interconnects for IC circuits; one step ohmic contacts; localized protective coatings; localized coatings for waveguide optics; and localized wear and corrosion resistant coatings.

Acknowledgments

This work was supported in part by a grant from AFOSR under the technical cognizance of H. Schlossberg.

REFERENCES

1. S. D. Allen, J. Appl. Phys. 52, 6501 (1981).
2. J. Cl. Puippe, R. E. Acosta, and R. J. von Gutfeld, J. Electrochem. Soc. 12, 2539 (1981).
3. D. J. Ehrlich, R. M. Osgood, Jr., and T. F. Deutsch, IEEE J. Quant. Elec. QE-16, 1233 (1980).
4. V. Baranauskas, E. I. Z. Mammana, R. E. Klinger and J. E. Greene, Appl. Phys. Lett. 39, 930 (1980).
5. S. D. Allen, A. B. Trigubo, and M. L. Teisinger, J. Vac. Sci. Tech. 20, 469 (1982).
6. C. F. Powell, J. H. Oxley and J. M. Blocher, Jr., Vapor Deposition Wiley, New York, (1966).
7. R. K. Sheline and K. S. Pitzer, J. Am. Chem. Soc. 72, 1107 (1950).
8. W. F. Edgell, W. E. Wilson and R. Summitt, Spectrochim. Acta 19, 863 (1963).
9. Organic Synthesis Via Metal Carbonyls, ed. I. Winder and P. Pino, Wiley, New York (1968).
10. American Institute of Physics Handbook, ed. by D. E. Gray, McGraw-Hill, New York, (1972).
11. J. A. Thornton, J. Vac. Sci. Technol. 11, 666 (1974).
12. L. H. Jones, Spectrochim. Acta 19, 329 (1963).
13. J. F. Ready, Effects of High-Power Laser Radiation Academic Press, New York, (1971).
14. S. D. Allen, unpublished.

$$Fe(CO)_5 \xrightarrow{370°C} Fe + CO$$

$$W(CO)_6 \xrightarrow{350°C} W + CO$$

$$WF_6 + H_2 \xrightarrow{600°C} W + HF$$

RELATIVE T_s FOR $WF_6 + H_2$ LCVD

P (WATTS)	T (MSEC)	$P\,T^{\frac{1}{2}} \propto T_s$
4.7	55.8	35.1
7.0	22.5	33.2
10.0	10.9	33.0
15.0	4.9	33.2

Table 2. Relative Surface Temperature, T_s, for Different Irradiation Conditions (W from $WF_6 + H_2$).

RELATIVE T_s for $WF_6 + H_2$ LCVD

P (watts)	t (msec)	$P\ t^{\frac{1}{2}} \propto T_s$
4.7	55.8	35.1
7.0	22.5	33.2
10.0	10.9	33.0
15.0	4.9	33.2

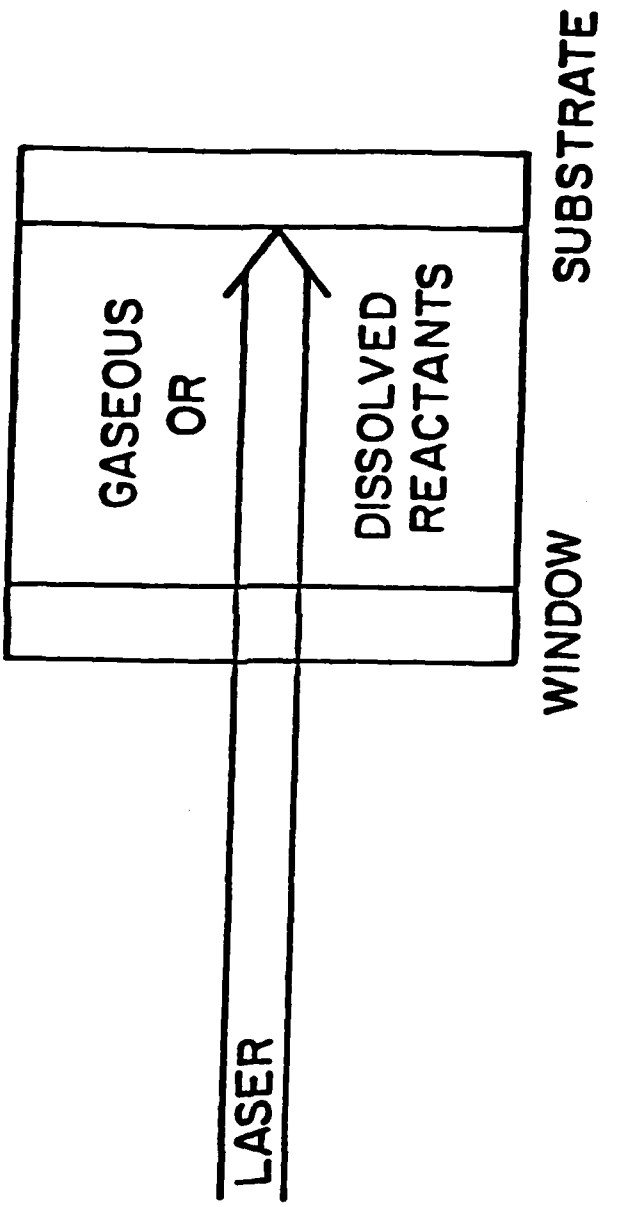
SUBSTRATE
GASEOUS
OR
DISSOLVED
REACTANTS
WINDOW
LASER

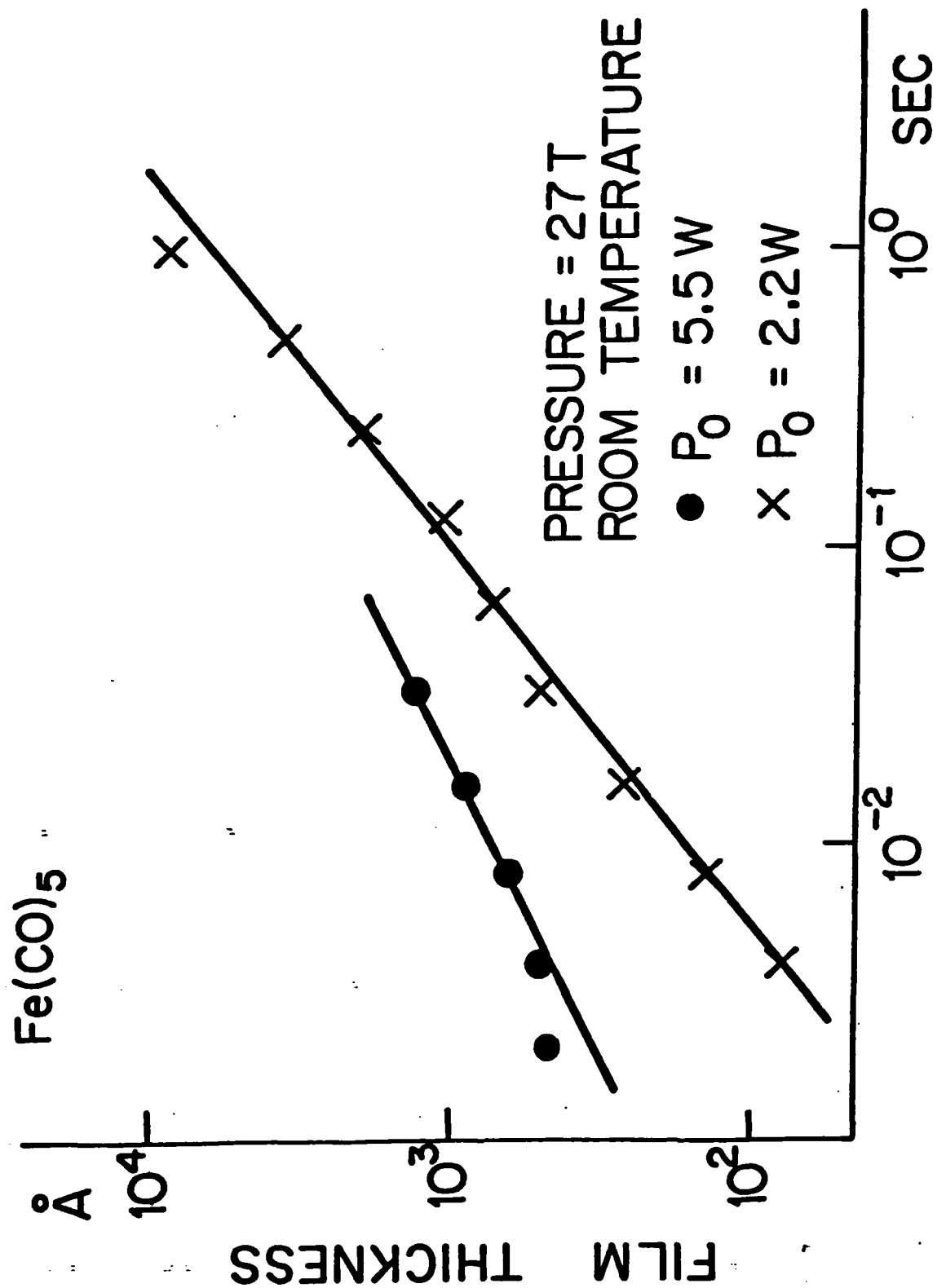
FILM THICKNESS
Å
10^4
10^3
10^2
$Fe(CO)_5$
PRESSURE = 27 T
ROOM TEMPERATURE
● P_0 = 5.5 W
× P_0 = 2.2W
10^{-2}
10^{-1}
10^0
SEC

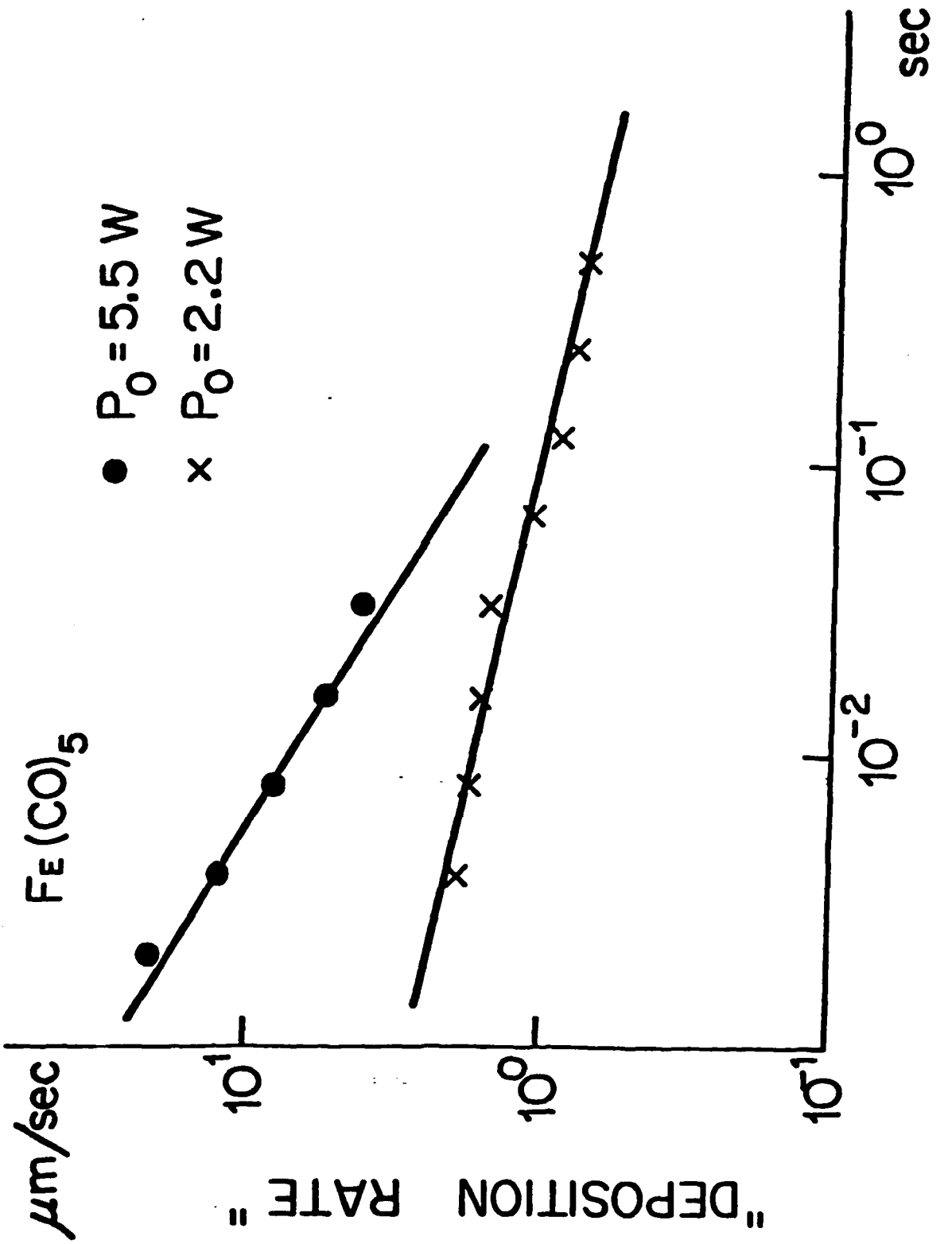
"DEPOSITION RATE"
μm/sec
10^{1}
10^{0}
10^{-1}
10^{-2}
10^{0}
10^{-1}
sec
$Fe(CO)_5$
● P_o=5.5 W
× P_o=2.2 W

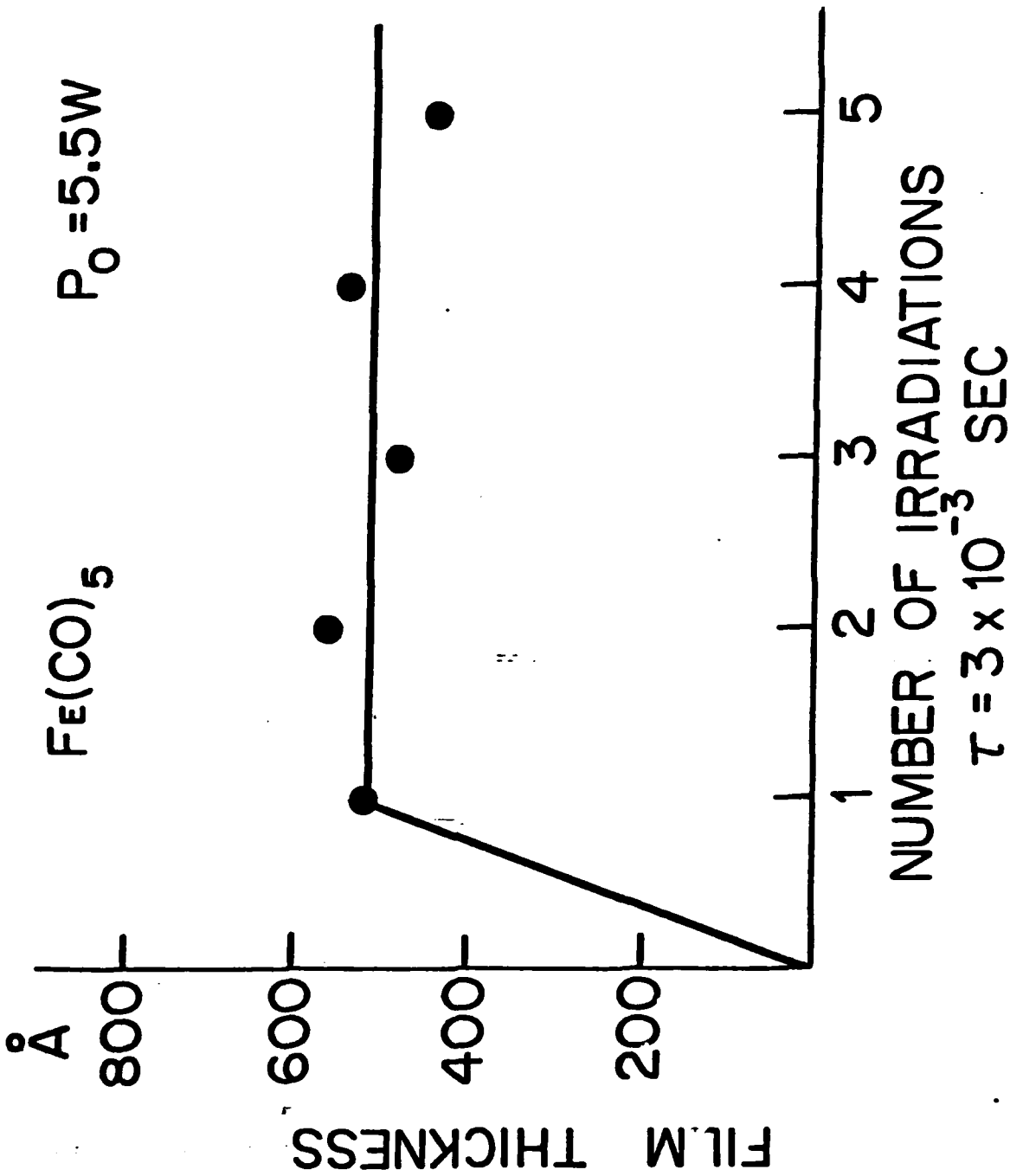
FILM THICKNESS
Å
800
600
400
200
1
2
3
4
5
NUMBER OF IRRADIATIONS
τ = 3 x 10⁻³ SEC
Fe(CO)5
P0 = 5.5W

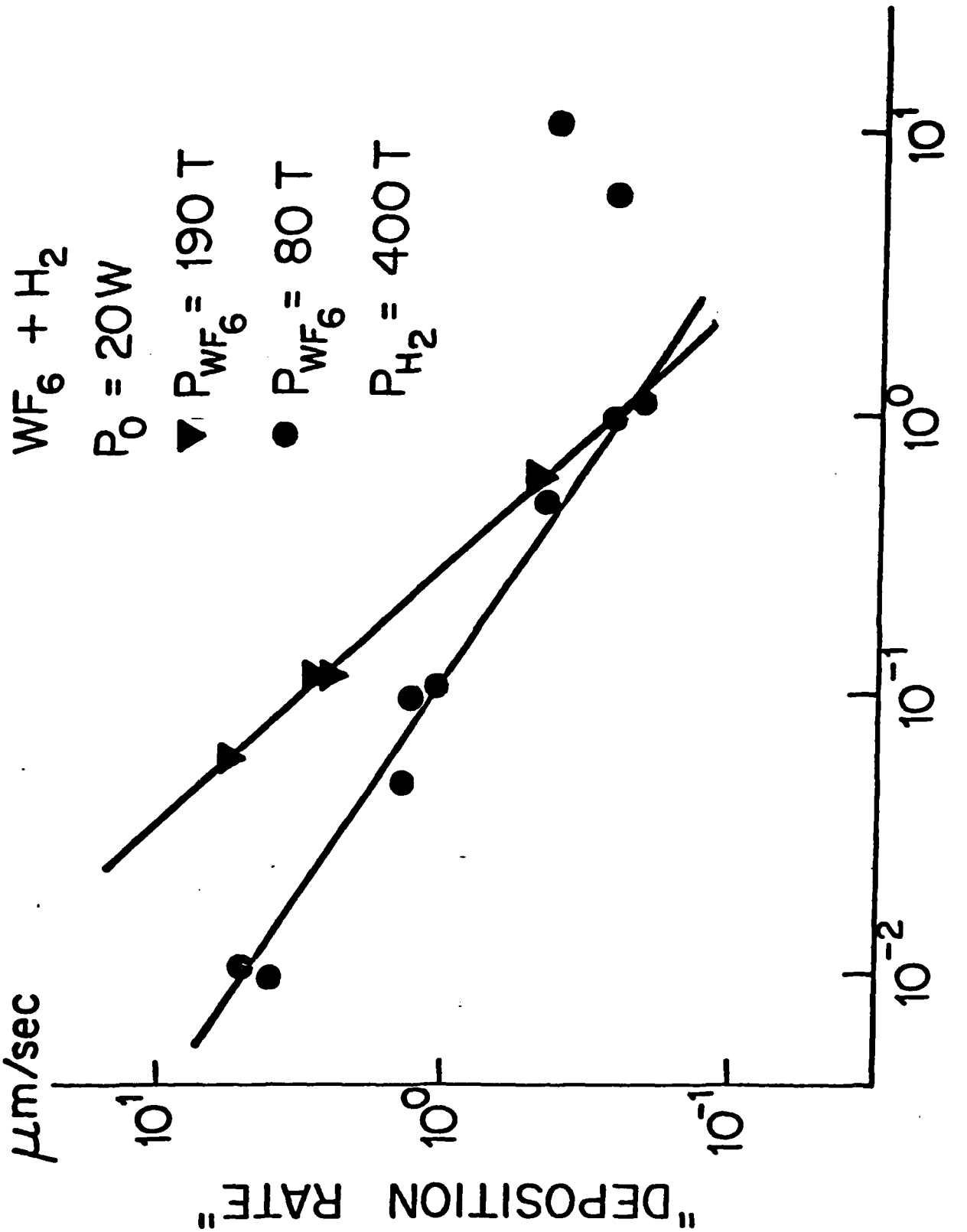
WF6 + H2
P0 = 20W
▶ PWF6 = 190 T
● PWF6 = 80 T
PH2 = 400 T
"DEPOSITION RATE"
μm/sec
10^1
10^0
10^-1
10^-2

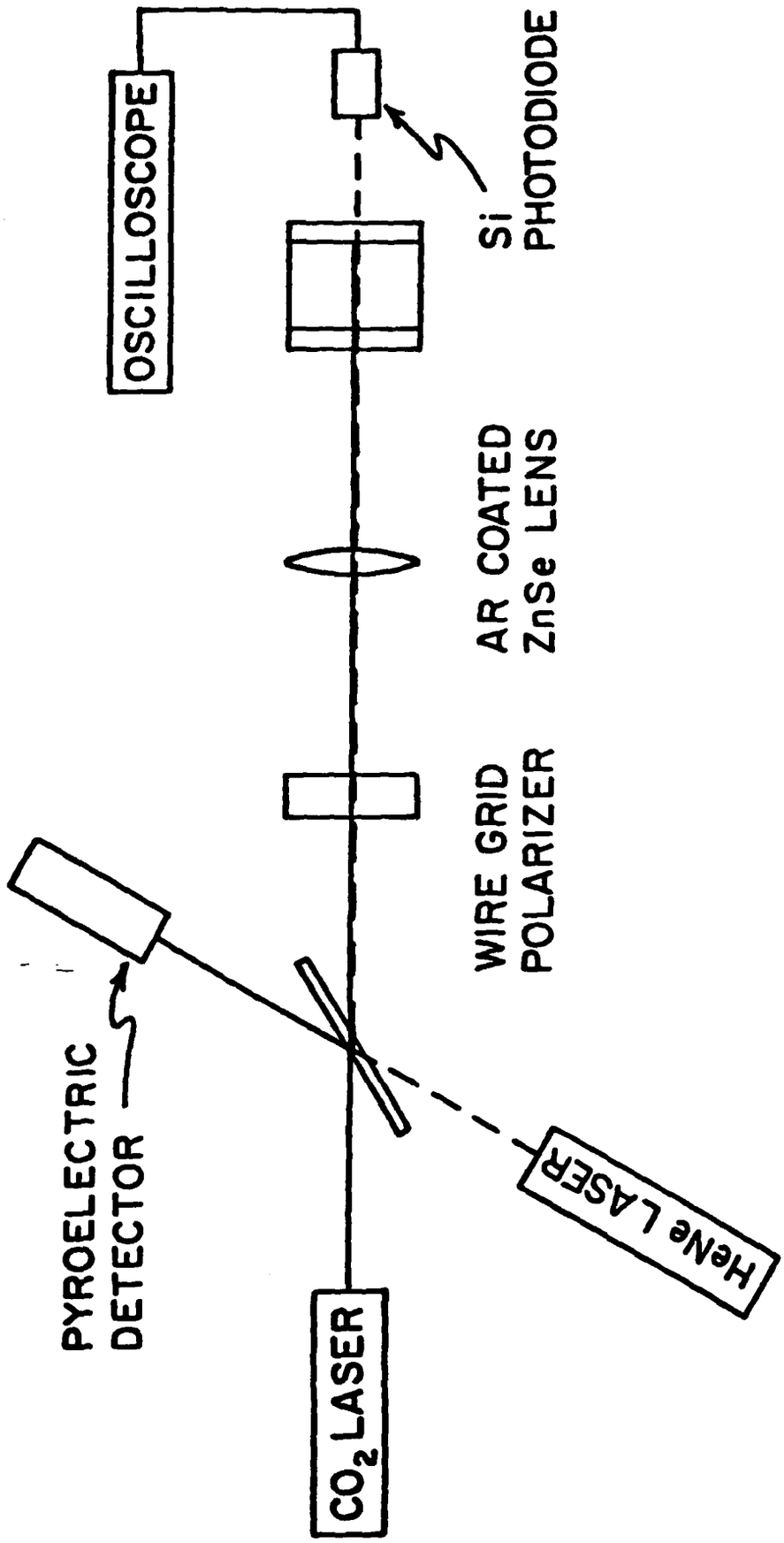
OSCILLOSCOPE
Si
PHOTODIODE
AR COATED
ZnSe LENS
WIRE GRID
POLARIZER
PYROELECTRIC
DETECTOR
HeNe LASER
CO_2 LASER

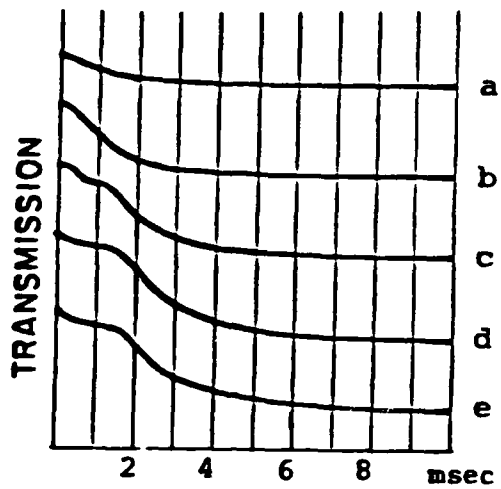
TRANSMISSION
a
b
c
d
e
2
4
6
8
msec

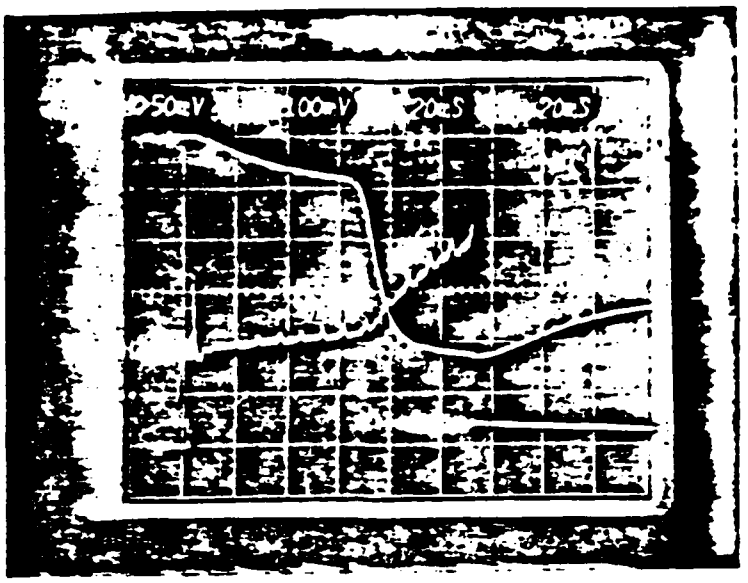

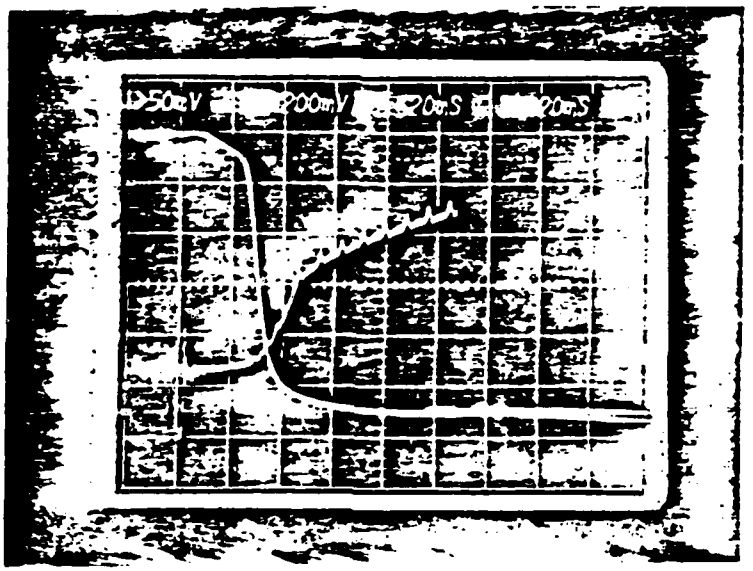

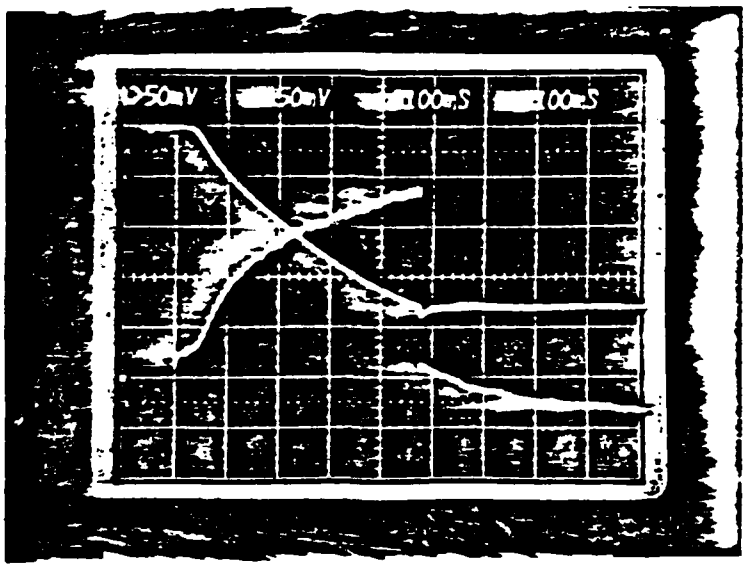

FIGURE CAPTIONS

Fig. 1. Generalized laser deposition experimental arrangement.

Fig. 2a. LCVD film thickness as a function of irradiation time (Fe from $Fe(CO)_5$ system).

Fig. 2b. Apparent deposition rate (film thickness/irradiation time) as a function of irradiation time (Fe from $Fe(CO)_5$).

Fig. 3. LCVD film thickness for multi-irradition sites (Fe from $Fe(CO)_5$). (Each data point is a separate site).

Fig. 4. Apparent deposition rate (film thickness/irradiation time) as a function of irradiation time (W from $WF_6 + H_2$).

Fig. 5. Pulsed LCVD apparatus.

Fig. 6. Transmission vs. time curves for pulsed LCVD of Ni from $Ni(CO)_4$ (40 T). Laser energy: a) 0.038 J; b) 0.051 J; c) 0.063 J; d) 0.076 J; e) 0.082 J. (Curves are offset for clarity).

Fig. 7a,b. Transmission and reflection vs. time curves for cw LCVD of W from $WF_6 + H_2$ (45 T, 400 T). The upper curve is the He-Ne transmission intensity and the lower curve the CO_2 reflected intensity. Laser power: a) 4.7 W; b) 7.0 W.

Fig. 8. Transmission and reflection vs. time curves for cw LCVD of Fe from $Fe(CO)_5$ (27 T). The upper curve is the He-Ne transmission intensity and the lower curve the CO_2 reflected intensity. Laser power is 2 W.

FIGURE CAPTIONS

Table 1. Representative LCVD reactions.

Table 2. Relative surface temperature, T_s, for different irradiation conditions (W from $WF_6 + H_2$).

END

FILMED

3-84

DTIC